AIR BORDER

JOINT CZECH-POLISH MEASUREMENTS OF TRANSBOUNDARY TRANSPORT OF AIR POLLUTANTS

PŘEKRAČUJEME HRANICE
PRZEKRACZAMY GRANICE
2014—2020

EVROPSKÁ UNIE / UNIA EUROPEJSKA
EVROPSKÝ FOND PRO REGIONÁLNÍ ROZVOJ
EUROPEJSKI FUNDUSZ ROZWOJU REGIONALNEGO

VŠB TECHNICKÁ UNIVERZITA OSTRAVA

IMGW

BEZPEČNOSTNĚ TECHNOLOGICKÝ KLASTR


FRANTIŠEK

AIR BORDER

JOINT CZECH-POLISH MEASUREMENTS OF TRANSBOUNDARY TRANSPORT OF AIR POLLUTANTS

Collective of authors

This work could be published thanks to the AIR BORDER project number CZ.11.4.120/0.0/0.0/15_006/0000118, which was co-financed by the European Union from the Interreg V-A Czech Republic-Poland 2014-2020 programme, Crossing Borders, the European Regional Development Fund and the state budget of the Czech Republic and Poland.

Ostrava, 2020

PŘEKRAČUJEME HRANICE
PRZEKRACZAMY GRANICE
2014—2020

EVROPSKÁ UNIE / UNIA EUROPEJSKA
EVROPSKÝ FOND PRO REGIONÁLNÍ ROZVOJ
EUROPEJSKI FUNDUSZ ROZWOJU REGIONALNEGO

Irena Pavlíková
Daniel Hladký
Petra Šutarová
Petr Jančík
Dr Leszek Ośródka
Dr Ewa Krajny

Photography @ Jan Langer

Press MORAVAPRESS s.r.o.
Typesetting and design: Studio CMYK Ostrava
ISBN 978-80-248-4550-0

MSc. Irena Pavlíková
Assistant Professor at the Department of Industrial Environmental Protection and Research Fellow at the Joint Institute for Nuclear Research in Dubna, Russian Federation
(Chapters 1, 2, 3.1, 4.2, 7)

MSc. Daniel Hladký
Employee of the Ostrava branch of the Czech Hydrometeorological Institute and researcher at the Department of Environmental Protection in Industry
(Chapter 7)

MSc. Petra Šutarová
Assistant professor at the Department of Industrial Environmental Protection and researcher at the Institute of Environmental Technology
(Chapters 1, 2, 8)

Associate prof. Petr Jančík, Ph.D.
Head of the Department of Environmental Protection in Industry and Senior Scientist at the Joint Institute for Nuclear Research in Dubna, Russian Federation

Dr Leszek Ośródka
Researcher of AIR BORDER project for Institute of Meteorology and Water Management - National Research Institute, Department of Air Pollution Modelling in Katowice
(Chapters 3.2, 4.1, 5, 6)

Dr Ewa Krajny
Researcher of AIR BORDER project for Institute of Meteorology and Water Management - National Research Institute, Department of Air Pollution Modelling in Katowice
(Chapters 3.2, 4.1, 5, 6)

Acknowledgements

We would like to thank the entire team from the Neutron Activation Analysis and Applied Research Sector, the Frank Laboratory of Neutron Physics, and the Joint Institute for Nuclear Research in Dubna, Russia, for their collaboration on the project and the implementation of the neutron activation analysis. In particular, Prof Marina V. Frontasyeva for her leadership of the implementation team, Dr. Sergey S. Pavlov for methodological guidance of the neutron activation analysis, and the implementation team, namely Pavel S. Nechoroshkov, Konstantin N. Vergel, Ludmila P. Strelkova, Tatyana M. Ostrovnaya and Margarita S. Shvetsova. We would also like to thank the NOAA Air Resources Laboratory (ARL) for providing the HYSPLIT transport and dispersion model and the READY website (https://www.ready.noaa.gov) which we have used in this work.

The authors would also like to thank the Main Inspectorate for Environmental Protection (Główny Inspektorat Ochrony Środowiska /GIOŚ/) for providing the data obtained in the during the fulfilling of the tasks for the State Environmental Monitoring (Państwowy Monitoring Środowiska /PMŚ/) performed by the authorities of the Inspectorate for Environmental Protection (Inspekcja Ochrony Środowiska /IOŚ/).

Research work financed from funds for science in the years 2018-2020 allocated for the implementation of an international project co-financed.

CONTENT

1 FOREWORD

Air pollution in the Czech-Polish border area of the Moravian-Silesian Region and the Silesian Voivodeship has been exceeding the limit values (LV) for a long time and thus represents a significant problem for human health and quality of life. This region is historically very closely associated with coal mining and heavy industry, represented mainly by power, coke and steel plants (Klusáček 2005; Cabala et al. 2004). The specific industrial character of the region and its topography, together with local meteorological conditions (Blažek 2013), causes its specific air pollution problems. The strategic industrial development of the region in the 1950s initiated intensive population growth, also associated with significant pollution emissions from local household heating (Hůnová 2020; Kuskova et al. 2008). This effect has persisted to the present day, as coal is still the most used fuel in the Polish border region (Ďurčanska 2020; Główny Urząd Statystyczny / Statistics Poland 2019). This makes the area one of the most polluted in Europe (European Environment Agency 2019). According to European legislation (European Council 2008) and World Health Organization (WHO) guidelines (World Health Organization 2006; Maynard et al. 2017), air pollution significantly exceeds the limit values for suspended particles (PM_{10}, $PM_{2.5}$), benzo[a]pyrene and ozone (European Environment Agency 2019; Czech Hydrometeorological Institute 2019; Hůnová 2020).

Daily and long-term exposure to the above mentioned pollutants brings together a number of confirmed adverse effects on human health (World Health Organization 2016; 2013). Increased levels of suspended particules in the air result in increased mortality and morbidity, even in case of short-term exposures. Populations exposed to dust particules/particulate matter (PM) have a higher incidence of infectious diseases (World Health Organization 2016; 2013; Jiřík et al. 2016), and suspended particulate air pollution is a factor classified as a proven human carcinogen (category 1) (Cohen et al. 2013). Considering the high population density of the region in question (Moravian-Silesian Region - 221 inhabitants per km^2 and Silesian Voivodeship - 366 inhabitants per km^2 as of 2019), high air pollution represents a major and long-term environmental problem.

The deteriorating air quality in the region is thus a long-term challenge for researchers to identify the specific causes of pollution and propose solutions to this unsatisfactory situation. In the 1990s, these efforts were kicked off by the US Environmental Protection Agency (US EPA) project „Silesia“ (Pinto et al. 1998; Cižová 1994); later efforts continued in the international projects „AIR SILESIA“ (Jančík et al. 2013) and „AIR TRITIA“ (Jančík et al. 2020). In addition, a number of case studies have been conducted on the origin of pollution (Mikuška et al. 2015; Pokorná et al. 2015; Leoni et al. 2018), including a recently published study by the Czech Hydrometeorological Institute (CHMI) (Czech Hydrometeorological Institute 2019; Seibert et al. 2020). All studies emphasised the role of industry and transboundary transfer of pollution from Poland to the Czech Republic, mainly originating from local heating. According to these studies and the results of state air quality monitoring (Czech Hydrometeorological Institute 2018; 2016), the highest PM concentrations on the Czech side occur near the Polish border (characterised by a more distinctive increase in the colder half of the year and during smog events) and also near major industrial sources, where PM limit values are exceeded not only during the winter season.

The air quality in the Czech part of the region is thus significantly affected by the speed and nature of transboundary transfer of pollution along the axis of the prevailing wind direction (typically SW / NE), together with the inverse nature of the weather with stable atmospheric layering, and thus the deteriorated dispersion conditions, which significantly contribute to increased air pollution during the winter season. According to the available studies (Ďurčanská 2020; Seibert et al. 2020; Volná and Hladký 2020), the contribution of transboundary pollution to annual average PM values on the Czech territory can vary between 20-40% depending on the location within the region, emissions and meteorological conditions of a given year.

The air quality monitoring presented in this monography was carried out within the framework of the international project „AIR BORDER“, focused particularly on the transboundary transfer of pollution from Poland to the Czech Republic and vice versa. Its aim was to carry out a special monitoring campaign to characterize the transfer of PM_{10} from different groups of air pollution sources specific to a given region, excluding the influence of local sources (Volná and Hladký 2020). This assumption was met by placing one of the monitoring devices on top of a tower that reaches a height of over 85 m above the ground. The unique device samples PM_{10} particles depending on the wind direction, which made it possible to investigate from which directions and from which sources air pollution originates and to quantify its transfer within the region more precisely.

2 ABOUT THE PROJECT

International project AIR BORDER - full name „Joint Czech-Polish measurements of transboundary transfer of air pollutants.“ - was supported by the Interreg V-A Czech Republic - Poland programme and co-financed by the European Regional Development Fund. The project ran from 2017 to 2020 and involved three partners. The lead partner of the project was the VŠB - Technical University of Ostrava (VŠB-TUO), another Czech partner was the Safety Technology Cluster, z. s. (BTK) and the Polish partner was the Institute of Meteorology and Water Management - State Research Institute (IMWM-SRI). The project activities were directed to the Czech-Polish border area, which is described in more detail in the following chapter.

On the basis of the established cooperation between Czech and Polish experts, specialised measurements were carried out within the project, the main objective of which was to characterise and quantify the transboundary transfer of PM_{10} pollution in the area of interest. The amount of transboundary transfer is also expressed by means of a directional vector displayed online on the AIR BORDER project website http://airborder.vsb.cz and in a mobile phone application. Another measurement objective was to determine the influence of different air pollution sources groups on long-term concentrations of PM_{10} pollution. Two monitoring stations, each on one side of the border, were used to implement these project objectives.

The station on the Czech side of the border was built with the financial support of the project in Horní Suchá at the former mining tower of the František Mine and measurements were made in the near-surface layer of the atmosphere at the base of the tower and then at about 90 m above the ground on the roof of the tower. Continuous measurements of suspended particulate matter were carried out at both altitudinal levels, and PM_{10} was also sampled on the tower roof as a function of wind direction. The collected PM_{10} particles were characterised using neutron activation analysis. For the measurements on the Polish side of the border, the existing measurement station in Racibórz was used, which was extended within the project with additional specialised equipment, namely a radiometer for measuring the vertical temperature profile and a ceilometer for measuring cloud base height, cloud amount, vertical visibility and aerosol concentration in the ground layer.

At the end of the project, the results of the measurements were compiled and summarised in a final paper on transboundary pollution transfer. The target groups of the project (governments, air protection authorities and civil society) on both sides of the border thus have data on how air pollution moves across borders and from what sources it mostly originates.

3 AREA OF INTEREST

The area of interest is situated in the Czech-Polish border in the north-East of the Czech Republic. It covers the areas of the Moravian-Silesian Region and the Silesian Voivodeship. See Figure 1.

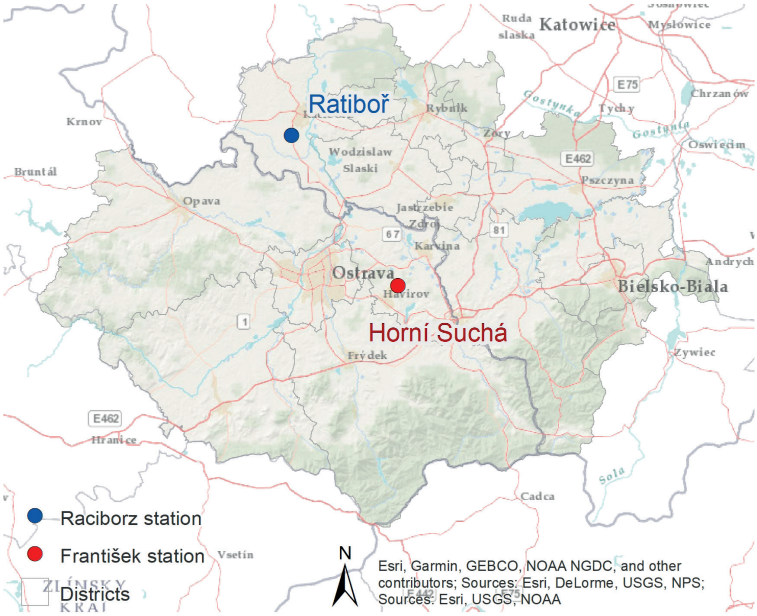

Figure 1: Definition of the project area of interest with the location of the measuring stations

3.1 Characteristics of the Czech part of the interest area

The Czech part of the interest area is defined by the administrative districts of Frýdek-Místek, Karviná, Nový Jičín, Opava and Ostrava-city.

3.1.1 Area topography

In the interest area, there are all types of terrain profile – the lowlands, hills, highlands and mountains. The highest part is the mountain range of Beskids mountains rising in the south east of the area. It is formed by the mountains over 1 000 m a. s. l. high with the highest peak of Lysá Hora at 1324 m.a.s.l. The lowest point of the area is near the Czech-polish border in the vicinity of conclusion of Odra and Olza rivers at the height of 192 m.a.s.l. (Moravian-Silesian Region 2021)

3.1.2 Area geomorphology

In terms of geomorphology, the area in the south-east is formed by the Western Carpathians, which are bordered by the Beskids mountain flysch massif and the adjacent foothills of the Moravian-Silesian Foothills. The centre of the area is represented by the Central European Lowland province, starting with the Moravian Gate, which stretches from the south-west in the form of a faulted depression formed by the broad floodplain of the meandering Oder River and opens wide towards Poland in the northeast in the form of the Ostrava Basin. This part of the region, rich in coal deposits in the past, gave historically rise to the industrial character of the region. In the west, the area passes into the Bohemian Highlands and rises to the Low Jeseníky Mountains.

Thanks to the mineral wealth, the area of interest became one of the most important industrial centres of the Czech Republic. However, the presence of high quality coking coal and the development of related industry were also closely linked to environmental pollution and irreversible changes to the landscape. Although there has been a significant decline in mining in the area (only one active mine in the Karviná region remains in operation today), traces of mining activity will remain in the landscape for a long time to come.

3.1.3 Area climate

The climate in the area is temperate with a typical change of four seasons. According to the Köppen classification (Kottek et al. 2006; Czech Hydrometeorological Institute and Palacký University in Olomouc 2007), most of the area belongs to the climate group Cfb - temperate oceanic climate, where the average temperature in the coldest month does not fall below 0°C, throughout the year the average monthly temperatures are below 22°C and at least 4 months above 10°C. No significant difference in precipitation is expected between seasons in this climate group. Part of the area covered by the Beskids and Low Jeseníky mountains falls into the Dfb - warm-summer humid continental climate with warm summers (with similar climatic characteristics to Cfb) and a small part of the Beskids peaks falls into the Dfc - subarctic climate group (with cool summers and cold winters). According to the observations of the Czech Hydrometeorological Institute (CHMI), the annual normal rainfall (1981-2010) in the area varies between 600-1,200 mm (depending on altitude), which is significantly higher than the Czech average.

3.2 Characteristics of the Polish part of the interest area

The Polish part of the area of interest is delimited by the administrative districts of Bielsko, Cieszyn, Pless, Racibórz, Rybnik, Wodzisław and administrative municipal districts of Bielsko-Biała, Rybnik, Jastrzębie-Zdrój and Żory.

3.2.1 Area geomorphology

The Polish part of the study area covers the territory of three macro-regions. These are the Silesian Lowland, which covers almost the entire territory of the municipality of Racibórz, and two mesoregions: the Opava Upland (Płaskowyż Głubczycki) and the Racibórz Basin (Kotlina Raciborska). Within the Silesian-Cracow Highlands macro-region (Wyżyna Śląsko – Krakowska), the Rybnik Plateau mesoregion (Płaskowyż Rybnicki) partially extends to the south-eastern border of Racibórz. The Ostrava Basin macro-region covers more than 600 km² (approx. 130 km² in Poland). It is heavily urbanised and industrialised. The surface is flat, sometimes hilly. It is bordered by the Silesian Lowland to the north-west, the Silesian-Cracow Highlands to the north-east, the Oświęcim Basin (Kotlina Oświęcimską) to the east, the Western Beskids Mountains to the south-east, the Moravian Gate to the south-west and the Polish Sudetenland to the west. In this area lies the station Horní Suchá.

3.2.2 Area Topology

The Racibórz Basin is in the most south-eastern part of the Silesian Lowlands (Kondracki 2014). It is adjacent to geographic units that rise significantly above the basin floor, so it has distinct and sharply defined boundaries. In the north, it is defined by the Chełm ridge (wzniesienie), which is part of the neighbouring Silesian Highlands/Upland (Wyżyna Śląska) - it reaches an altitude of 400 m above sea level (St. Anna Mountain / Góra Świętej Anny). To the east it borders with the Rybnik Plateau (280-310 m above sea level), which is also part of the Silesian Highlands. On the opposite, western side, it borders with the Opava Upland, which lies at an altitude of 250-300 m above sea level. It is open only to the south and is connected to the Ostrava Basin via the Upper Oder Basin. The valley floor, 4-5 km wide, lies on average 100-200 m lower than the peaks of the adjacent highlands and plateaus. The Racibórz basin widens to the north and takes the shape of an isosceles triangle. This basin belongs to the Silesian-Welkopolska Lowlands.

3.2.3 Area climate

The local climate is warm, with long summers, with temperatures around -2°C in January and 18°C in July. Winter lasts 60-80 days and summer about 100 days. The average rainfall is 600-700 mm. The climate of the Racibórz Basin is mainly influenced by the influx of warm, from south coming airflow through the Moravian Gate and from the west from the Silesian Plain. According to E. Romer's division of the area into climatic regions (Romer 1949), Racibórz lies in the climatic zone ‚Moravian Gate', which is one of the warmest climatic zones in Poland, with the longest growing season. The Racibórz basin has relatively mild meteorological conditions, it is warmer here than in the surrounding geographical regions, especially in the Silesian Highlands. A strong influence on these climatic conditions, especially on the wind structure situation, is the shape of the basin, which is mainly manifested in the airflow. The location of Racibórz in the Oder valley, the proximity of the mountain ranges and the Moravian Gate cause the transfer of pollution from the area around Ostrava. In addition, the shape of the Oder valley makes it prone to the accumulation of polluted air due to frequent inversions.

4 MEASURING STATIONS

Within the AIR BORDER project, air pollution by suspended particles and meteorological data were measured at stations on both sides of the border in the most polluted part of the area of interest. On the Czech side the measurements were carried out at the newly built station in Horní Suchá, on the Polish side at the existing IMWM station in Racibórz. The location of the measuring stations within the region is shown in Figure 2.

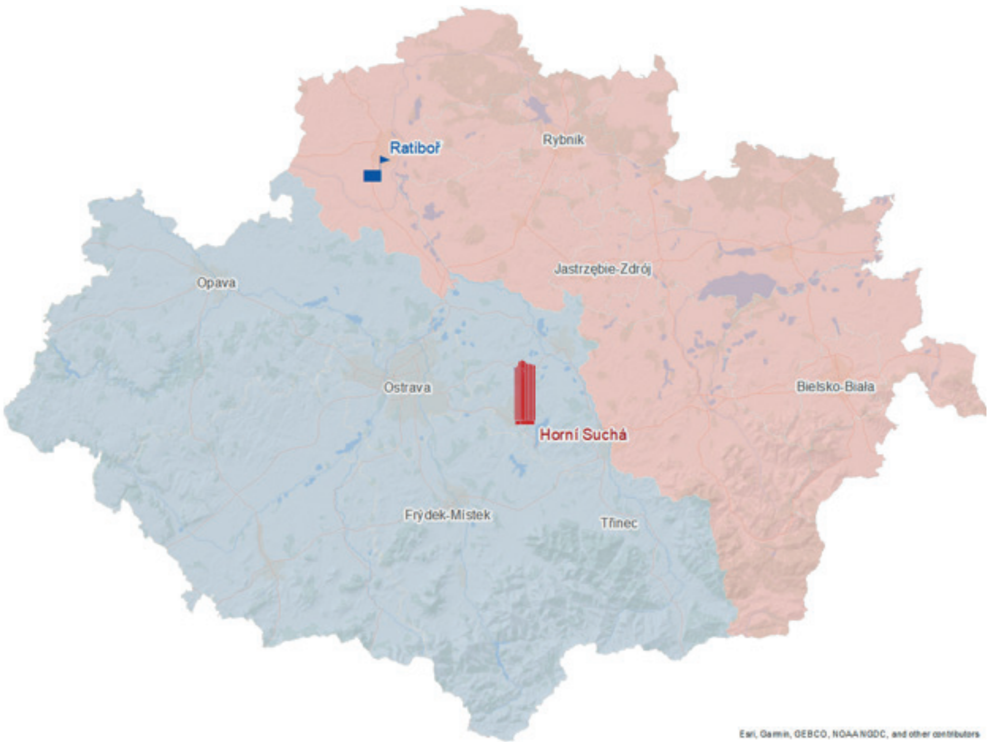

Figure 2: Location of measurement stations in the area of interest

4.1 Racibórz Monitoring

The station in Racibórz carries out specialised meteorological and air quality measurements focused on monitoring of atmospheric aerosol. During the implementation of the AIR BORDER project, the station was expanded to include continuous measurements of the vertical temperature profile in the atmospheric boundary layer using a radiometer and measurements of aerosol layer deposition using a ceilometer to identify the inversion layer of air pollution dispersion. The application in the measurement programme of the radiometric station and the equipment for identification of the temperature distribution in the atmospheric boundary layer is an important element in the identification of the actual transfer of pollutants across the Polish-Czech border. The station can be seen in Figure 3.

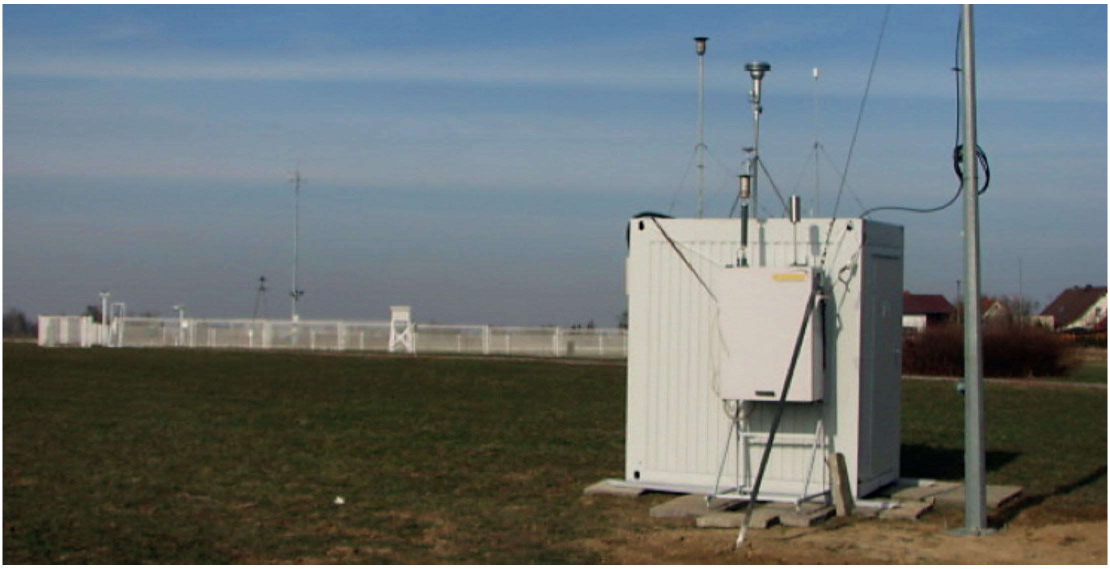

Figure 3: Station IMWM-SRI in Racibórz

4.1.1 Locality description

The measuring station in Racibórz is located in the geographical macroregion of the Silesian Lowland, between its most southeastern mesoregions, the Racibórz Basin and the Opava Hills, at an altitude of 206 m above sea level (Kondracki 2014). The relief shows a transitional character between lowland and highland. The Racibórz basin is a tectonic pre-Carpathian depression filled with clays and sands, through the centre of which runs the upper Odra riverbed at an elevation range of 180-185 m above sea level. The rectilinear course of this channel on the SSW-SSE axis follows the course of the tectonic fault. Several terrace levels occur on the 4-5 km wide floor of the Oder valley and on both its slopes. Along the western slope of the Oder valley, a small channel called the Psinka runs parallel to the main course of the river. Detailed hypsometric conditions can be seen in Figure 4.

The station in Racibórz Studzienna measures air quality and is located on the territory of the hydrological and meteorological station of category I of IMWM -SRI, at a distance of about 200 m from the meteorological garden in the SW direction, at a distance of about 4 km to the SW from the centre of Racibórz. The station is adjacent to the east by a strip of suburban housing in the southern part of the Studzienna district. The strip of this development stretches along the exit road from Racibórz to Chałupki. On the western side there are wide-open fields stretching towards the village of Krzanowice. On the southern side there are first open fields, which are closed at a distance of 0.8 km by the suburban development of Sudołu, another district of Racibórz, which lies about 5 km from the town centre.

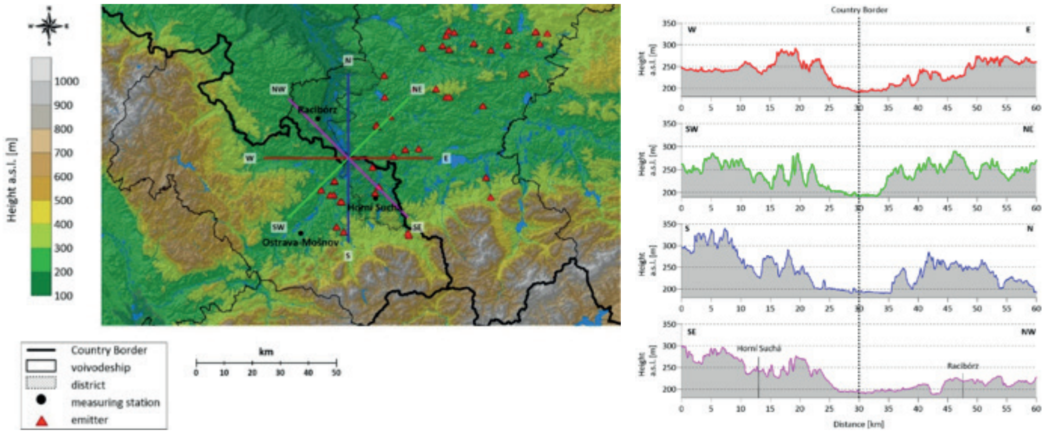

Figure 4: Location of the IMWM-SRI station in Racibórz - hypsometric profiles at a distance of 10 km in each of the main directions, the central point is the location of the radiometer, the dashed line is the PL-CZ state border.

4.1.2 Measuring Equipment

The basis for information on meteorological data is the measurement programme according to the standards of the World Meteorological Organization (WMO) of the synoptic station IMWM-SRI Racibórz Studzienna. The station is equipped with an automatic measurement system - the Vaisala MAWS-301 weather station together with a set of meters, sensors and detectors. See Figure 5 (a)

The basic measurement range of the aerosol monitoring station includes:

- Measurement of the number and mass concentration of aerosol particles (see Figure 5 (d)):
  - Aerodynamic Particle Sizer Spectrometer (APS),
  - Ultra Fine Particle Monitor (UFP),
  - Dust Track (DRX) dust monitor.
- Aurora 3000 integrated nephelometer (Ecotech) for the measurement of optical air parameters (3 wavelength ranges) - nephelometer measurements are used, among other things, to investigate the effect of aerosols on optical air parameters and visibility.
- Aerosol deposition measurements using the Vaisala CL31 ceilometer (see Figure 5 (b)).
- Measurement of vertical air temperature distribution using the MT-5 radiometer (see Figure 5 (c)).

Fig. 5: Location of measuring equipment at the meteorological and aerosol monitoring station in Ratibor Studzienna: (a) meteorological garden; (b) ceilometer; (c) radiometer; (d) aerosol measuring container.

The results of the aerosol and weather measurements at the station, obtained using the above measurement equipment, were used to carry out the research tasks of the project. A model of the thermal conditions of the atmosphere stratification developed on the basis of the results of measurements of the MPT-5 radiometer located on the roof of the weather station at a height of 12 m above the ground was also used for the research.

The measurement system at the IMWM-SRI meteorological station in Racibórz (PL) was integrated with measurements of meteorological conditions and air pollution in Horní Suchá (CZ) from the measurement station of the VŠB-TUO. At both sites, data on air pollution by suspended PM with fractions from 0.03 to 20 μm were recorded. A schematic of the integrated data collection is shown in Figure 6.

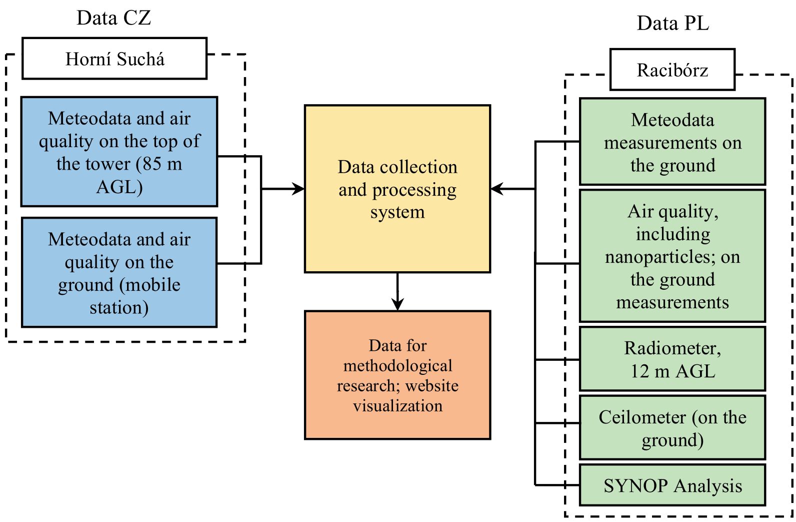

Figure 6: Block diagram of the meteorological monitoring and air quality monitoring system.

4.2 František Monitoring

On the Czech side, specialised measurements are being carried out in Horní Suchá at the former mining tower in the František industrial zone. WGS 1984 49.805166N, 18.473954E. The tower is located in the centre of the Ostrava-Karviná agglomeration, close to the border with Poland. This allows the investigation of pollution transfer from different groups of air pollution sources typical for the region. See Figure 7. The height of the tower allows measurements to be made almost 90 m above the ground, thus separating the influence of local pollution sources from the transmission over longer distances.

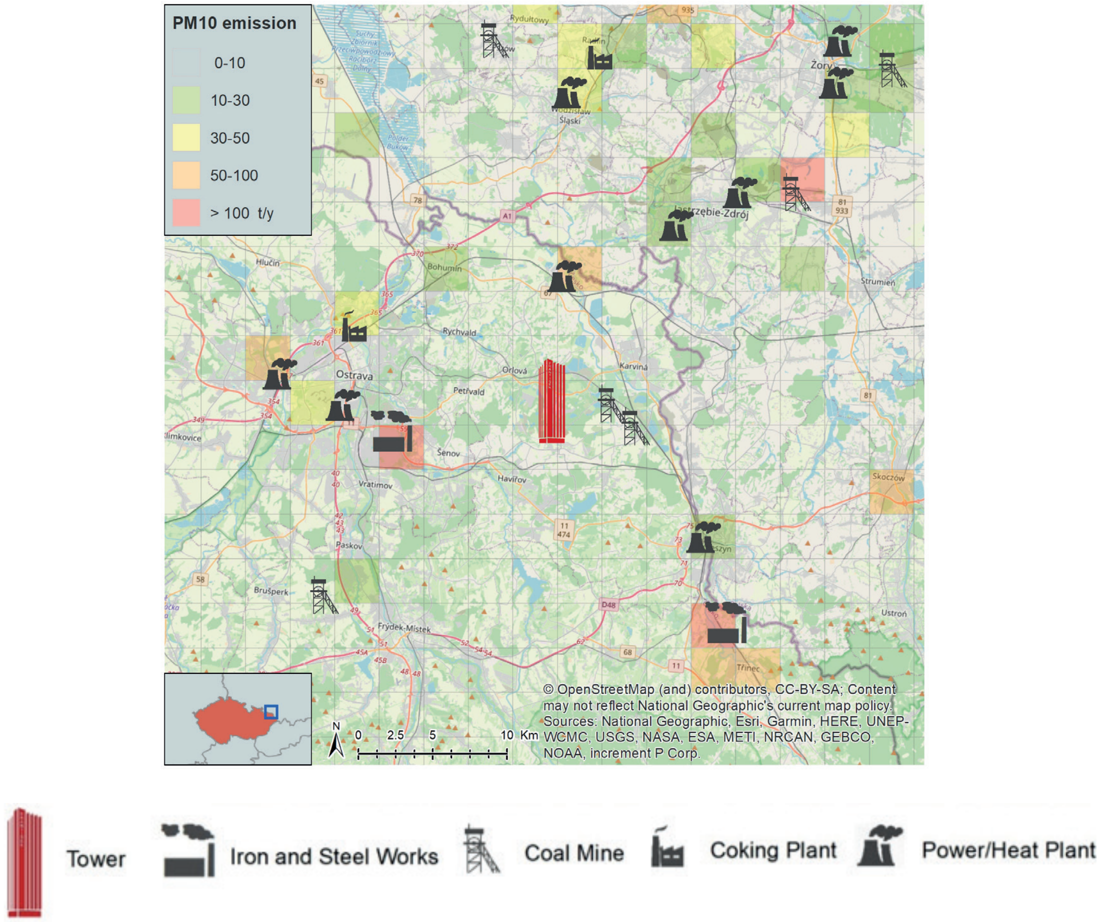

Figure 7: Location of the station František in the region with PM_{10} emissions determination from nearby industrial sources valid for 2018

4.2.1 Locality description

The mining (skip) tower with the original designation F4 operated as part of the František coal mine in Horní Suchá. See Figure 8. The beginning of mining in this mine dates back to 1911, when the first mining pit started to be dug, the last car was mined on 30 June 1999. Over its entire history, the mine has produced a total of 59,144,518 tonnes of hard coal. Most of the site has undergone significant transformation in the recent past. The original buildings and equipment of the mine were removed and the municipality of Horní Suchá turned the area into a modern industrial zone, retaining the original name of the mine: František.

The reinforced concrete mining tower covers an area of 586 m^2 and reaches a height of 85.5 m, so it could not be safely removed due to the surrounding housing estate. It remains an unmistakable dominant feature of Horní Suchá and a reminder of the rich mining history of the region.

The municipality is trying to find an alternative use for the tower, and so the idea of its involvement in the AIR BORDER project as a site for specialised measurements of air pollution transfer arose. As part of the project, the tower was fitted with measuring equipment for continuous measurement of suspended particulate matter and sampling of the PM_{10} fraction depending on wind direction.

Figure 8: View of the original František Mine site in the 1980s (zdarbuh.cz 2020)

4.2.2 Measuring equipment

At the base and on the roof of the tower (at a height of approximately 86 m above ground level), suspended particulate matter levels are measured continuously using the Fidas 200 S device (Palas GmbH, Karlsruhe, Germany). This is a standard automatic optical analyser capable of monitoring aerosol particles with a size range of 180 nm to 18 µm. It monitors concentrations of suspended particulate matter fractions PM_1, $PM_{2.5}$, PM_{10} and TSP.

In addition, a prototype device for wind-direction dependent PM_{10} sampling - the SAM Hi30 AUTO WIND high volume sampler (Baghirra s.r.o., Prague, Czech Republic) - is installed on the tower (at a height of about 90 m above the ground). This sampler was designed to determine the directions and sources of pollution and to quantify more accurately its further distribution within the region.

The sampler operates in accordance with the Compendium of Methods for the Determination of Inorganic Compounds in Ambient Air: Sampling of Ambient Air for Total Suspended Particulate Matter (SPM) And PM_{10} Using High Volume (HV) Sampler, developed by the US EPA (United States Environmental Protection Agency 1999); a summary of research on the effectiveness of bulk samplers can be found in the article (Krug et al. 2017).

The SAM Hi 30 AUTO WIND is a fully automatic remote-controlled sampler designed for gravimetric and chemical analysis of aerosol particles. The device collects particles with a diameter of <10 µm (PM_{10}) using a DIGITEL DPM10/30/00 PM_{10} sampling head (flow rates of 30 m^3/h) in accordance with the relevant standard EN 12341 (European Committee for Standardization 2014). The sampler has been designed to operate depending on weather conditions. It has a tray for 15 filters (glass microfiber, Whatman GF/A, Ø150 mm), which are in holders and automatically move to the sampling position according to the assessed wind conditions. The sampler is thus able to collect PM_{10} particles from eight basic wind directions (N, NE, E, SE, SW, W, NW) and calm (wind speed <0.2 $m.s^{-1}$). The sampler can be seen in Figure 9.

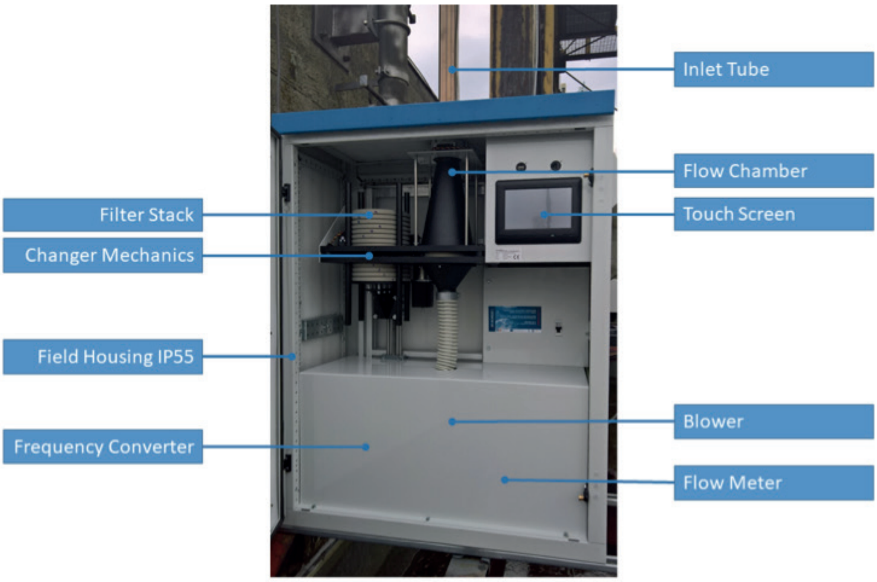

Figure 9: SAM Hi 30 AUTO WIND sampler

Wind speed and direction are measured using a WindSonic™ SDI-12 anemometer (Gill Instruments Limited, Hampshire, United Kingdom). Wind speed and direction for selecting a particular filter from the sampling stack are determined from hourly moving averages calculated from 10-minute data in accordance with U.S. EPA methodology (U.S. Environmental Protection Agency et al. 2000). In addition, one filter is designed for episodes of extreme air pollution, defined as three consecutive hourly average PM_{10} concentrations exceeding 100 µg.m^{-3} (determined from 10-minute ground-based monitoring data) - so-called smog situations.

Suspended particles samples are collected on the filters for one month at a time. They are then subjected to elemental analysis using neutron activation analysis in a nuclear reactor in Russia. The results of the elemental analysis then help determine the origin of the sampled particles.

5 WEATHER CONDITIONS IN THE INTEREST AREA

5.1 Long-term weather conditions

The assessment of meteorological conditions in the area of interest is based on long-term measurements from 2005 to 2019. Given the annual variability of weather, meteorological data obtained from the longest possible time series of measurements are more reliable. WMO recommendations are that such a series should be at least 30 years. In our case, the longest homogeneous series for the area, i.e. almost 15 years was used. The obtained results are representative for the climate in the area of interest.

The location of the measuring stations in the area of interest is specific; both stations are located in the lower part of the area, on the edge of the Ostrava basin in the Oder valley. Although the barrier between the Carpathians and the Sudetes represents the natural boundary of the climatic areas, for the purpose of this work and due to the short distance between the two measuring stations, it is assumed that their climatic conditions are similar and are represented by the meteorological station IMWM-SRI in Racibórz.

The climatological characteristics that have the most significant influence on the air quality in the area were chosen for the evaluation. The analysis of the climatic background of the study area was based on data from the IMWM -SRI meteorological station in Racibórz. The visualisation of monthly trends of selected climatic characteristics is presented in Figure 10 – Figure 21.

Monthly air temperatures in Racibórz are typical for areas that are located in temperate transition climate zones. The warmest month is July (19.8°C) and the coldest is January (-0.9°C). See Figure 10. The highest maximum temperatures observed at the site are in August (28.6°C) and the lowest minimum temperatures are in January (-22.4°C). See Figure 11 and Figure 12. This differs slightly from, for example, the Silesian Highlands, where the lowest temperatures are observed in February. In view of the measured values, it can therefore be concluded that the division of the year into a cold season (October-March) and a warm season (April-September) is justified.

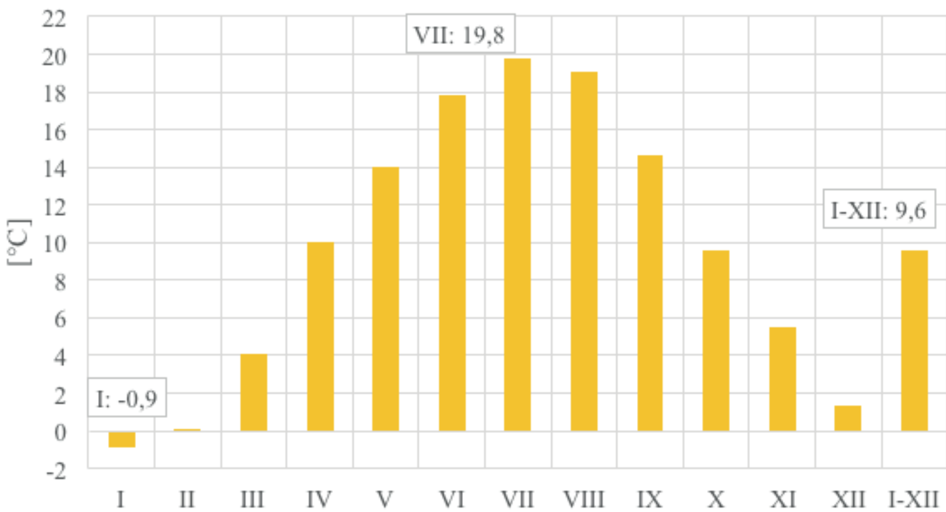

Figure 10: Average monthly air temperatures from 2005 to 2019

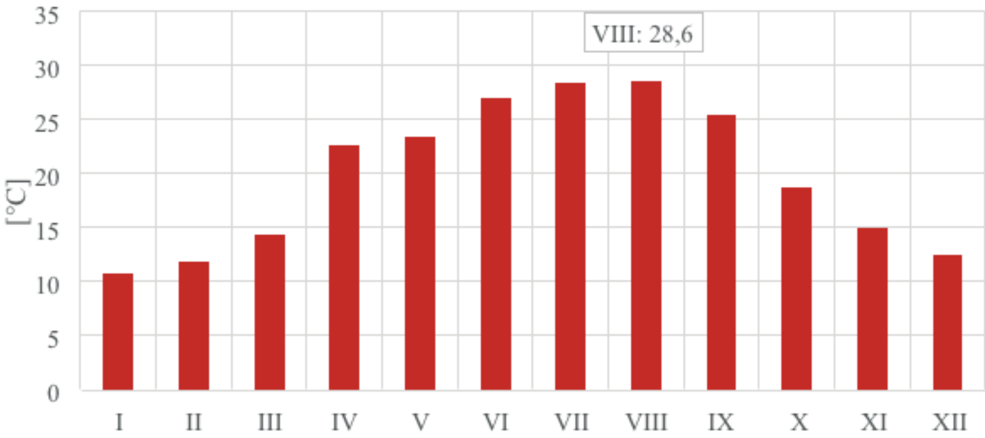

Figure 11: Maximum monthly air temperatures from 2005 to 2019

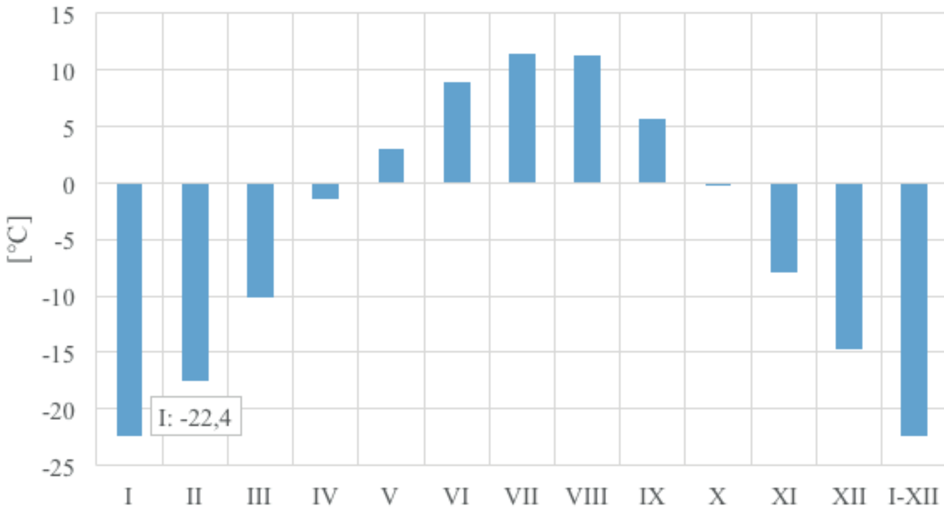

Figure 12: Minimum monthly air temperatures from 2005 to 2019.

The average sunshine time in hours depends on the length of the day and the total cloud cover. Therefore, the highest values are observed in July (267 hours) and the lowest in January (52.8 hours). See Figure 13.

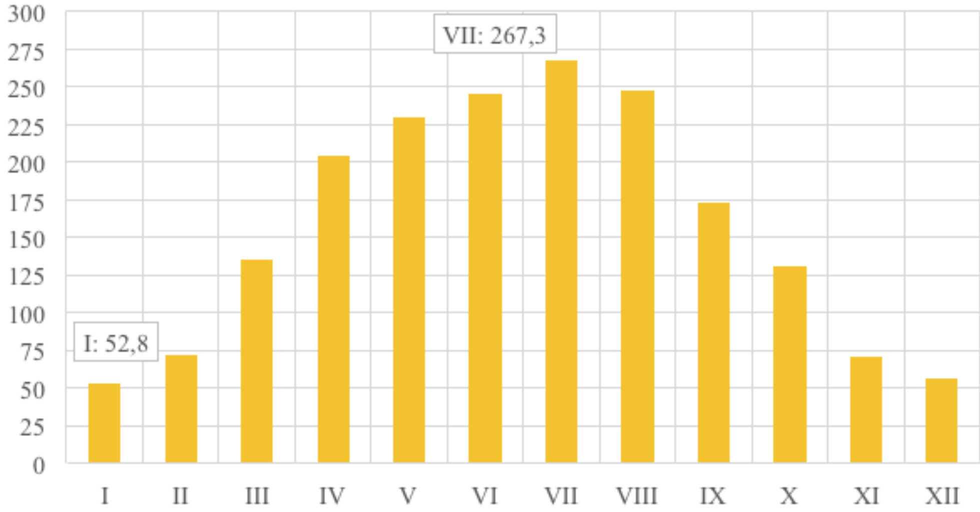

Figure 13: Average monthly values of total sunshine in hours (vertical axis number of hours) from 2005 to 2019, year I-XII: 1881 hours.

The measured monthly average atmospheric pressure values are typical for the transitional temperate zone. See Figure 14. The highest average measured pressure values occur in October (1019.2 hPa) and are the result of the occurrence of long-term pressure highs in this region. This also influences the airflow in the atmosphere here. The lowest pressure values fall for the summer period when there is an increased cyclonic activity, hence the minimum mean atmospheric pressure value of 1014.5 hPa observed in July, which is also reflected in the increased rainfall during this period.

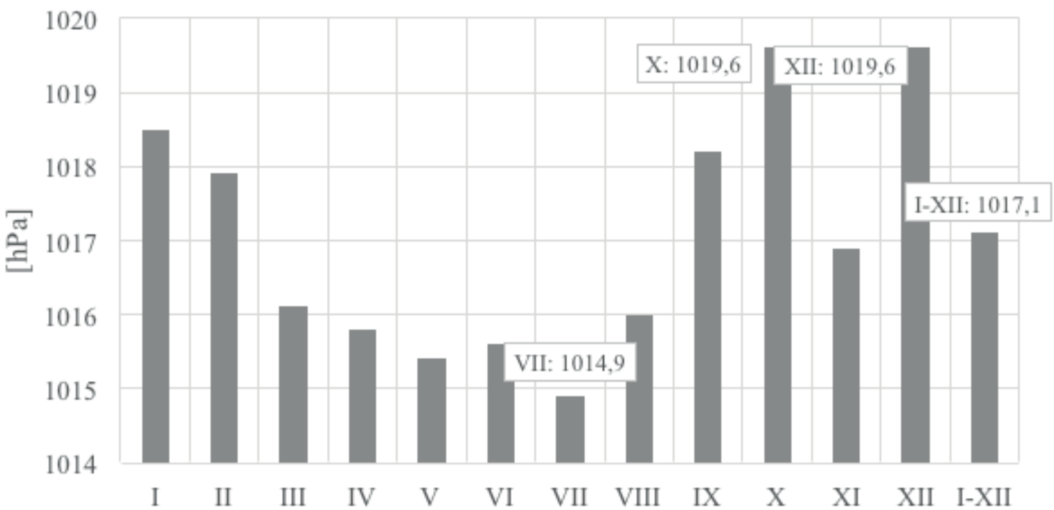

Figure 14: Average monthly sea level pressure values from 2005 to 2019.

Long-term values of average monthly precipitation are related to the typical transitional nature of temperate zones. It shows the characteristics of a continental climate with the highest precipitation in summer (convective precipitation). The total maximum rainfall is 79.9 mm in July and the minimum is 24.8 mm in February. See Figure 15.

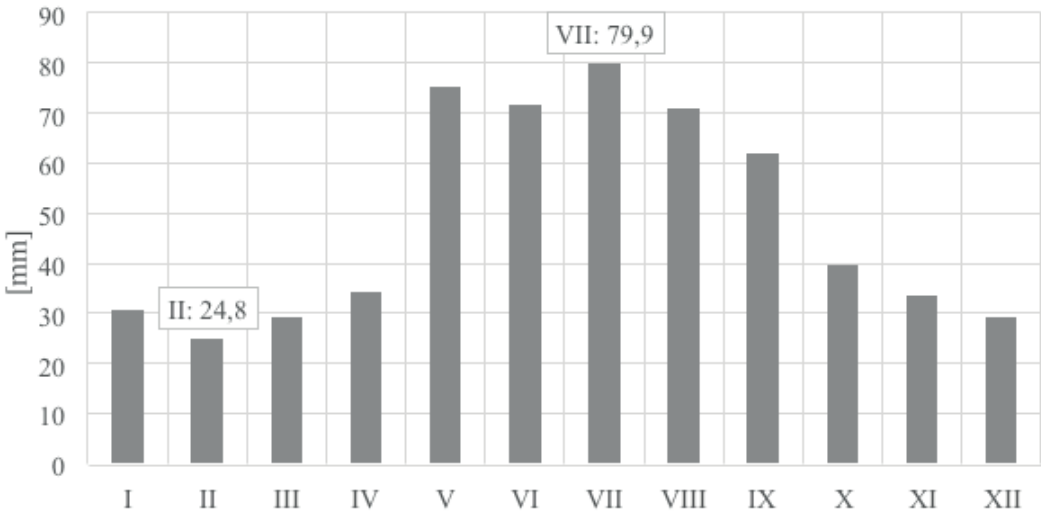

Figure 15: Average monthly precipitations from 2005 to 2019, year I-XII: 581.2 mm.

Maximum daily precipitation is most often found in the warm season (July: 63.4 mm) and is related to convective cloud cover. Maximum daily precipitation totals are lowest in the cold season: total values per day range from 20.9 mm in December to a minimum of 10.7 mm in January. See Figure 16.

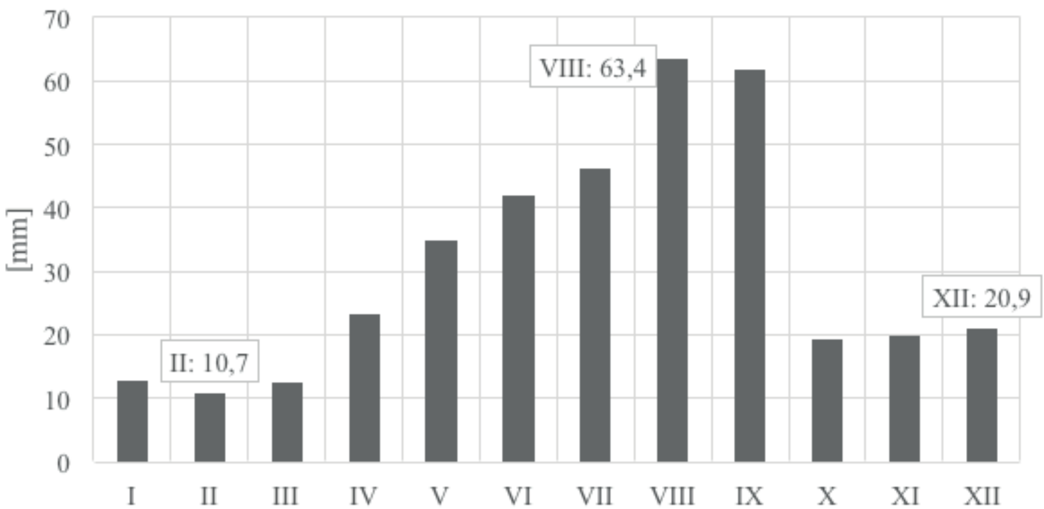

Figure 16: Maximum monthly precipitations from 2005 to 2019.

The number of days with precipitation (daily precipitation ≥ 0.1 mm) is typical for the temperate transition climate zone. The wettest month in terms of days of precipitation is January (16 days) and at the opposite pole is April (11 days). See Figure 17.

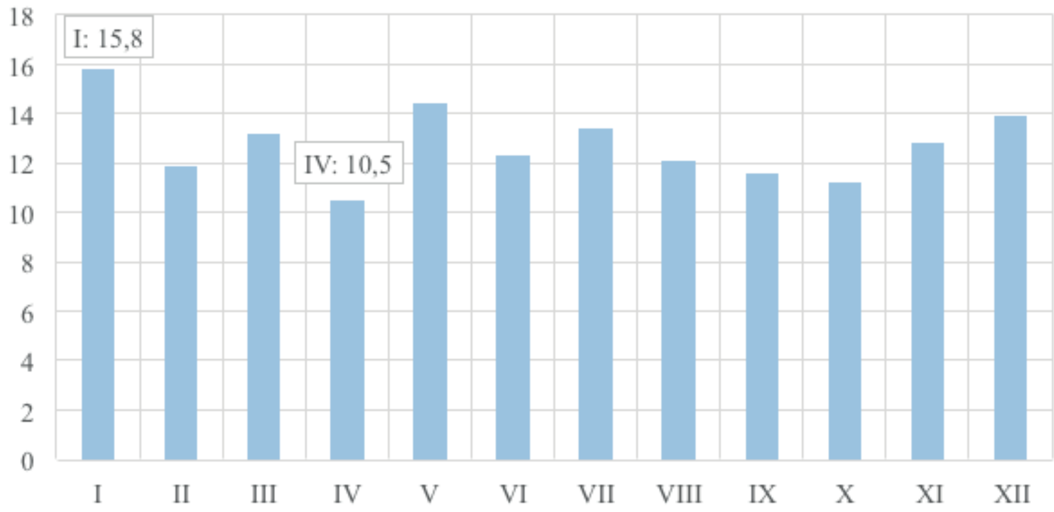

Figure 17: Monthly number of days with precipitation from 2005 to 2019, year I-XII: 153 days.

Snow cover is observed in Racibórz from November to March, exceptionally in October (0.1 day) and still in April (half a day). The number of days with snow cover averaged over the period is 43.9 days per year, of which the longest snow cover is in January (17 days). There is no snow cover from May to September. See Figure 18.

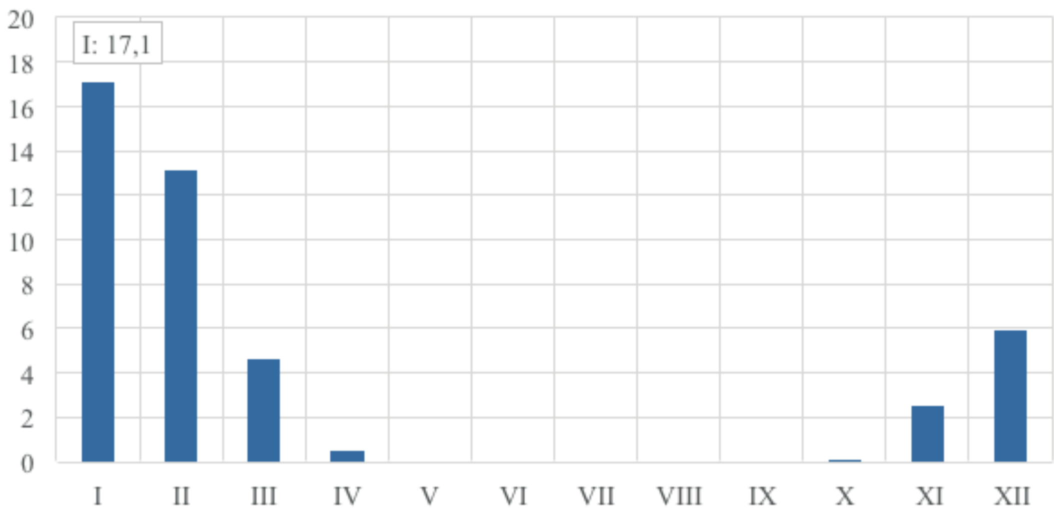

Figure 18: Monthly number of days with snow cover between 2005 and 2019. Vertical: number of days, year I - XII: 44 days.

Monthly average wind speeds reflect weather conditions typical of areas under the influence of a temperate continental transition zone. The lowest values occur in summer: in August, the average speed reaches a maximum of 2.8 $m.s^{-1}$. Significantly higher speeds occur in winter. The maximum average wind speed is in January and reaches 3.9 $m.s^{-1}$. See Figure 19.

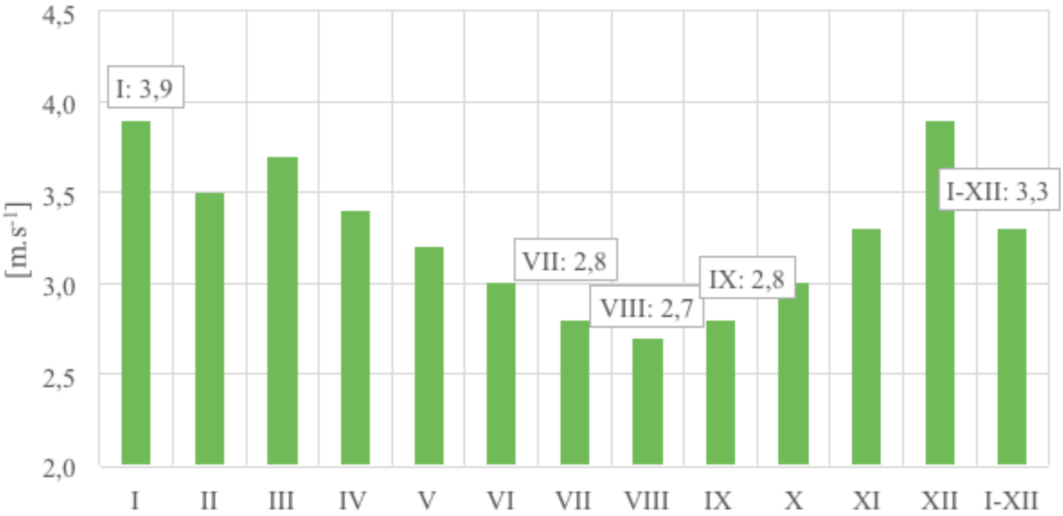

Figure 19: Average monthly wind speeds from 2005 to 2019.

The proportion of calm in the monthly graph shows that in no month does it exceed 5% of the time. Relatively high proportions of calm are visible from July to October (> 3%), with a maximum of 4.6% in October. Calm is least frequent in the first half of the year and least frequent in December: 1.9% of the time. On average, it accounts for 3% of all weather observations in a year. See Figure 20.

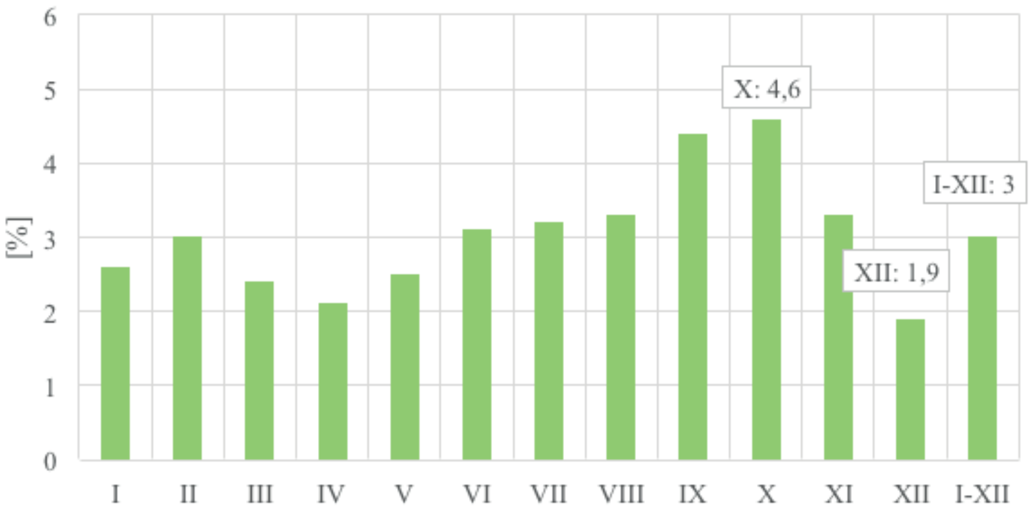

Figure 20: Monthly occurrence of calm (wind speed < 0.5 m/s) from 2005 to 2019.

The number of days with an average wind speed per day < 2 m.s^{-1} occurs most frequently in September (4 days) and October (3 days). Such days are least frequently observed from March to May with a minimum in April (less than 1 day). See Figure 21.

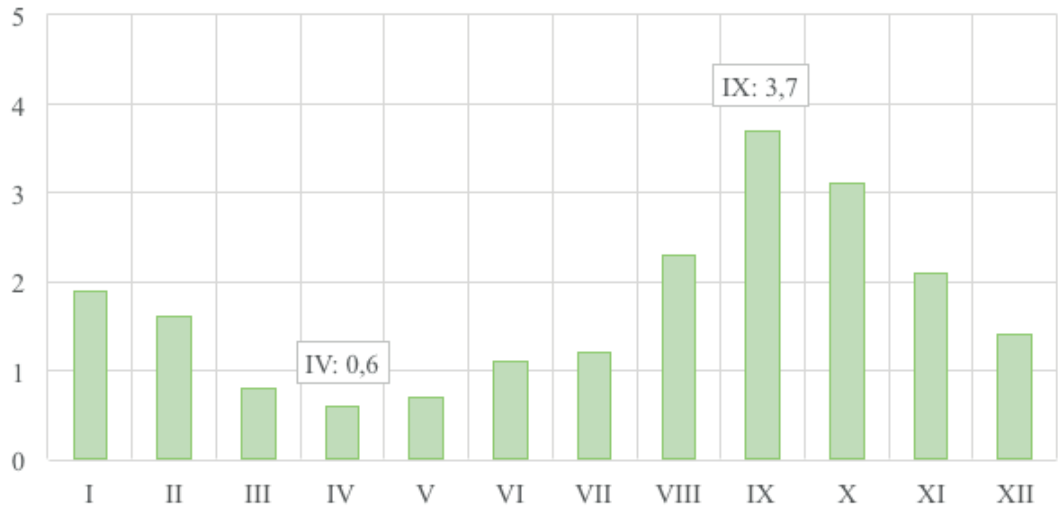

Figure 21: Monthly occurrence of low wind speeds (daily average < 2 m.s^{-1}) from 2005 to 2019; year I-XII: 20.5 days. Vertical - number of days.

The wind rose in Racibórz is under the influence of the general climatic circulation strongly modified by the shape of the terrain. Meridional directions (135-225° and 315-360° zones) prevail throughout the year, both in the cold and warm seasons, while in the heating season the directions from the south gain over the northern directions. See Figure 22.

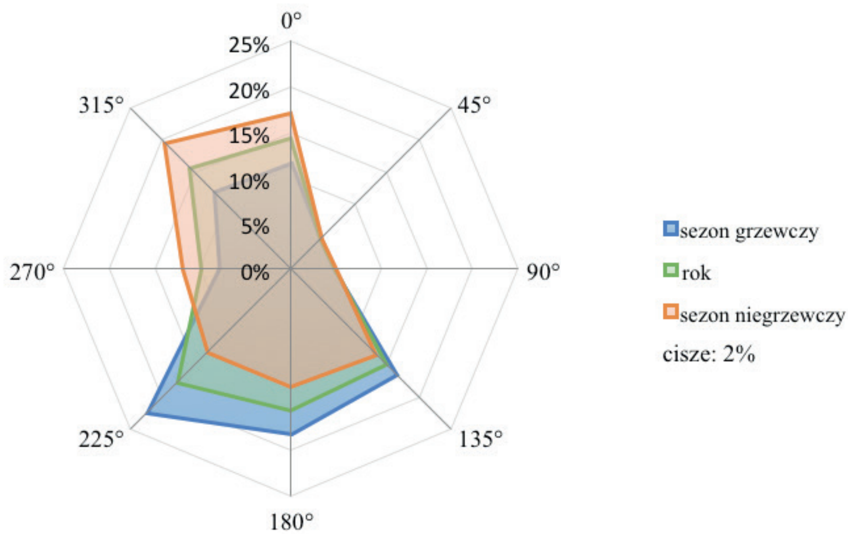

Figure 22: Wind rose in Racibórz for years 2005 – 2019.

5.2 Ventilation conditions in the atmosphere based on radiometric investigations

A parameter that expresses the distribution of temperature conditions in the atmosphere are the so-called temperature stratification classes. These classes capture the modelled pattern of the vertical temperature gradient in the ground-surface layer of the atmosphere obtained by a radiometer.

Based on empirical investigations, we distinguish 5 such classes. See Table 1.

Table 1: Distribution of temperature stratification classes according to radiometric measurements.

Temperature stratification class	Description of a layer distribution	Type of class stability in the ground level	Part of the day – highest occurrence
1	It is characterised by a normal temperature distribution with increasing height. No inversion occurs at any level - this class corresponds approximately to the unstable stratification of the atmosphere	Unstable	day
2	It is characterised by the occurrence of a small layer of inversion near the Earth‘s surface (about 50 m), and later by a normal temperature distribution	Inert	evening-night
3	It is characterised by a normal temperature distribution in a layer up to about 100 m above the ground, followed by inversions of much greater thickness (about 500 m) and then a normal distribution. This type of mixed stratification is typical of the so-called morning transition, when the surface of the earth, warmed by the sun‘s rays, transfers heat to the ground layer of the atmosphere	Little stable	morning
4	Ground-level inversion with a large temperature jump that extends to about 50 m above the ground, then a normal temperature distribution, and at 400 m above the surface a height inversion of about 300 m thickness. Above that, a normal distribution	stable	night
5	Strong inversion from the ground surface to a height of about 100 m; it is characterized by permanent stratification at the ground surface	Very stable	night

Averaged over the whole year, we observe a significant predominance of class 1 (normal temperature distribution from the ground surface) in the hours around noon. At night, class 5 (significant ground-level inversion) is most common. See Figure 23. These two classes significantly dominate the others, confirming Stull‘s theory of boundary layer structure evolution (Stull 1988).

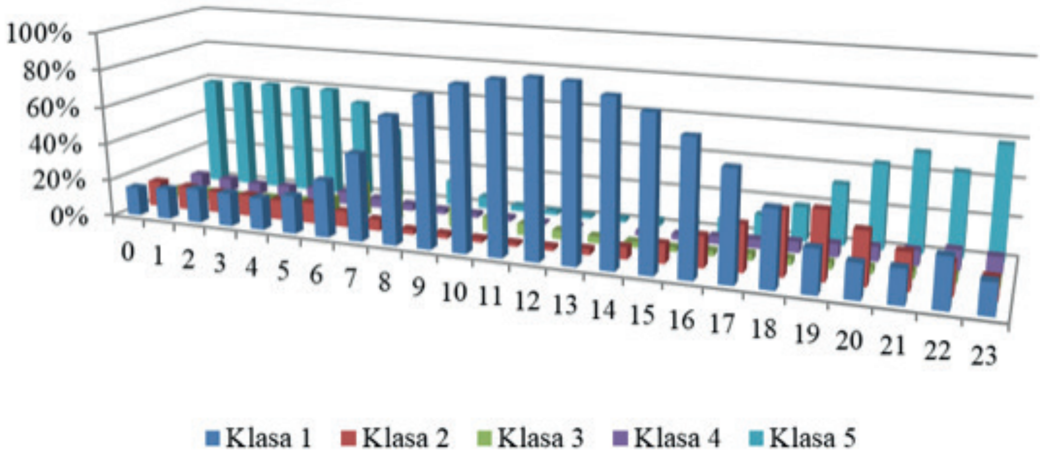

Figure 23: Daily course of temperature stratification classes in the upper Oder valley averaged over the year.

In the winter season, the diurnal pattern of the temperature stratification of the atmosphere (TSA) classes is characterized by a shorter duration of class 1 during the day and an increase in the proportion of classes 2-4, with an almost identical proportion of class 5. See Figure 24 and Figure 25.

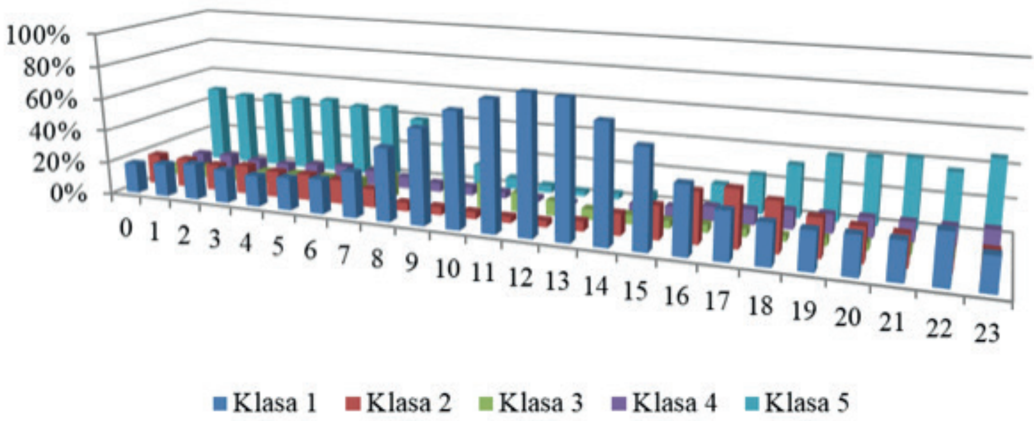

Figure 24: Daily temperature stratification in the upper Oder valley during the winter season (cold X-III).

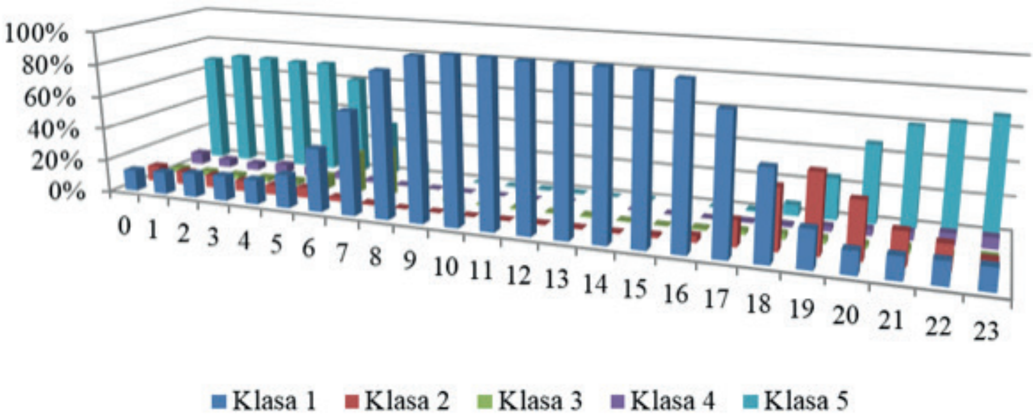

Figure 25: Daily temperature stratification in the upper Oder valley during the summer season (warm IV - IX).

The significance of the temperature stratification classes is also reflected in the observed PM_{10} concentrations. Comparisons were made for a one-day period. The average daily PM_{10} concentrations were compared with the percentage of each class on a given day. See Figure 26 and Figure 27.

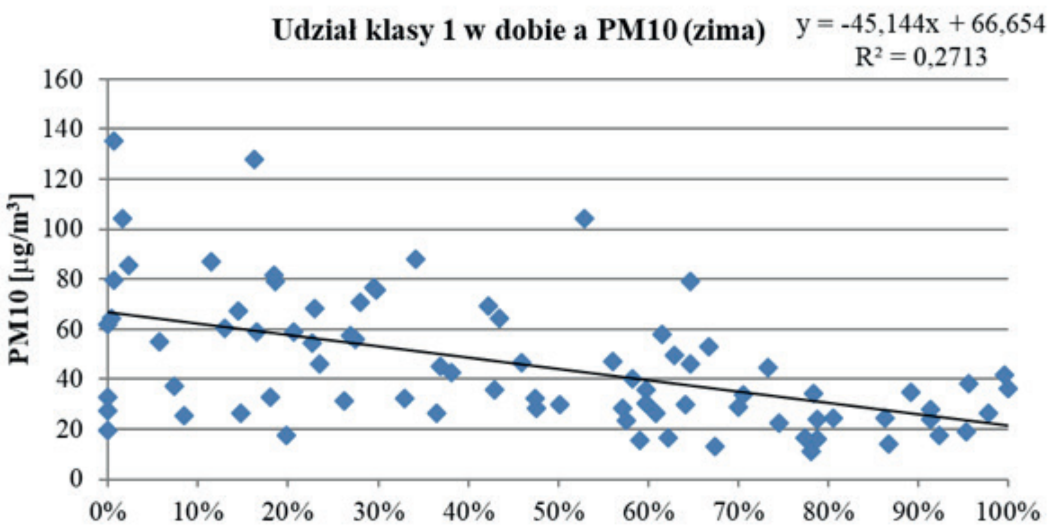

Figure 26: Daily Class 1 fraction and average daily PM_{10} concentrations - winter (cold part of year X-III).

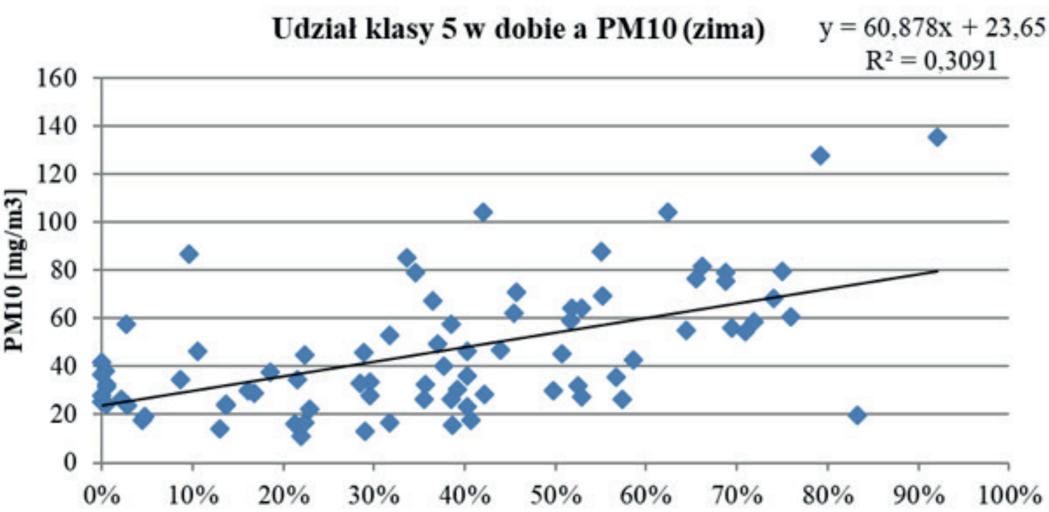

Figure 27: Daily fraction of Class 5 and average daily PM_{10} concentrations - winter (cold part of year X-III).

The obtained indications show that Class 1 and 5 are significantly related to the measured PM_{10} concentrations. The more Class 1 there is per day, the lower the PM_{10} concentration. For class 5 we observe the opposite situation.

Furthermore, the correlation of PM_{10} concentration, temperature stratification classes from radiometer and meteorological parameters measured at IMWM -SRI Racibórz Studzienna station was determined. The correlations are observed during the day period. See Table 2.

Table 2: Correlation of PM_{10} concentration, temperature stratification and meteorological conditions for one day.

Factor	**Correlation coefficient PM_{10}**
Class 1	−0,554
Class 2	−0,154
Class 3	0,183
Class 4	0,166
Class 5	0,496
T_{Max}	−0,335
T_{Min}	−0,464
T_{Avg}	−0,399
T_{MiG}	−0,458
Precipitations	−0,113
Raining time	−0,110
Raining time	0,188
Fog time	0,567
Haze time	0,613
Relative humidity	0,387
Wind speed	−0,354
Cloud base	0,175
Visibility	−0,718
Total cloud cover	0,018

Analysis of the results presented in Table 2 shows a significant correlation between the daily concentration of PM_{10} in Racibórz and TSA classes 1 (negative correlation) and 5 (positive correlation). It also shows a significant correlation between the daily concentration of PM_{10} and the following meteorological conditions: temperature and visibility characteristics (negative correlation), fog and haze periods (positive correlation). A slightly weaker relationship is observed with relative humidity (positive correlation) and wind speed (negative correlation). The duration of TSA classes 2 - 4 shows a weak association with the daily PM_{10} concentration.

The conducted analyses confirm the conclusions of previous research on the effects of meteorological conditions on suspended particulate matter concentrations. In case of stable weather in the sense of low typological variability (represented by classes 1 and 5), the relationships between meteorological conditions and particulate matter concentrations are significant. In case of variable weather, represented by TSA classes 2 to 4, the dependence is less significant.

The above described characteristics of scattering conditions in the atmosphere can be used if a radiometer is available. To evaluate the effect of these conditions in the earlier period, a different means was needed that was based on radiometric data from 2018-2020 and could be used retrospectively. Therefore, the multivariate analysis (clustering, Sammon projection) (Krajny a Ośródka 2020; Ośródka et al. 2018; Degórska et al. 2016) was used to evaluate the scattering conditions in the area of interest. By performing it, the dispersion conditions were grouped into groups called ventilation indexes (VI). First, the clustering of the vectors of hourly values of meteorological elements was performed and the average pollution concentrations were calculated for each group.

The following characteristics were typical for the groups with the highest pollution concentration values thus obtained:

- Low wind speed (instantaneous average < 2 m.s^{-1}),
- Low visibility, max 1,000 m,
- Presence of fog and haze,
- Complete inversion (thermal stratification class TSA 5).

For the sake of simplicity, 5 partial indexes (I) were allocated in a given observation hour:

$$I_1 = \begin{cases} 1 \; when\ the\ wind\ speed\ \leq 2\ m/s \\ 0\ in\ an\ opposite\ case \end{cases}$$

$$I_2 = \begin{cases} 1 \; when\ the\ wind\ speed = 0\ m/s \\ 0\ in\ an\ opposite\ case \end{cases}$$

$$I_3 = \begin{cases} 1 \; when\ visibility < 10\ km \\ 0\ in\ an\ opposite\ case \end{cases}$$

$$I_4 = \begin{cases} 1 \; when\ there\ is\ a\ fog\ or\ haze \\ 0\ in\ an\ opposite\ case \end{cases}$$

$$I_5 = \begin{cases} 1 \; when\ the\ stratification\ class = 5 \\ 0\ in\ an\ opposite\ case \end{cases}$$

Wind occurs in two indexes to emphasize its importance.

The total hourly index was then calculated from the formula:

$$I(h) = \sum_{k=1}^{5} I_k(h)$$

Since the pollution level is also influenced by the previous situation, the final ventilation index was determined as the sum of the last three hourly indexes:

$$VI(h) = I(h) + I(h-1) + I(h-2)$$

The classification according to the applied ventilation indices is given in Table 3.

Table 3: Quantification of the ventilation index (VI).

VI value	Characteristic	Flow class
0	no conditions for assessing dispersion are met	No class
1 – 3	good dispersion conditions	A
4 – 6	slightly unfavourable dispersion conditions	B
7 – 8	unfavourable dispersion conditions	C
9 – 12	poor dispersion conditions	D

Based on the above algorithm, ventilation indexes were determined for the period 2010-2019. Figure 28 shows the annual variation of the ventilation index corresponding to poor dispersion conditions (class D), showing a decreasing trend in its occurrence. This means that in recent years, more situations with more weather dynamics (fewer inversions) are observed and therefore there were fewer situations favouring high air pollution concentrations. This is particularly well seen in the years 2015-2019 (the best situation was in 2018 and 2019).

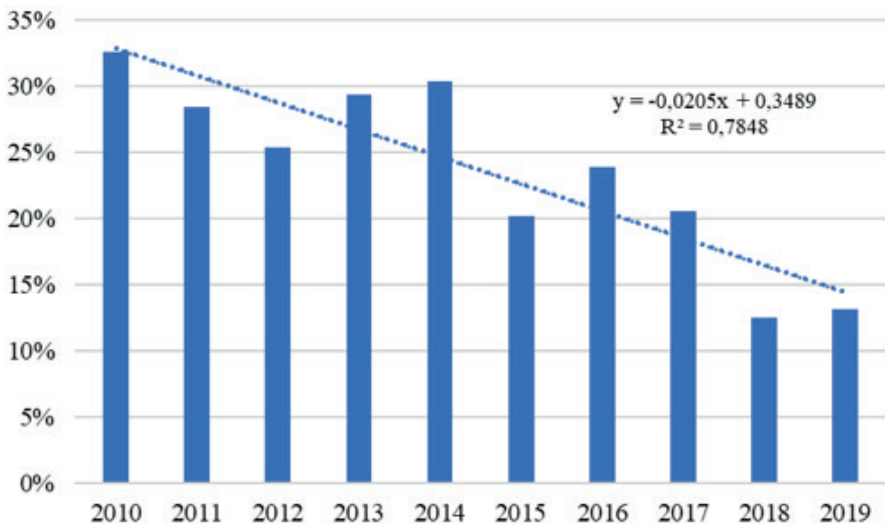

.

Figure 28: Proportion of VI with poor dispersion conditions - class D in 2010-2019.

5.3 Dispersion and wind conditions during joint measurements

The proportion of occurrence of each ventilation index in 2018 and 2019, i.e. during the joint project measurements, is shown in Figure 29 and Figure 30.

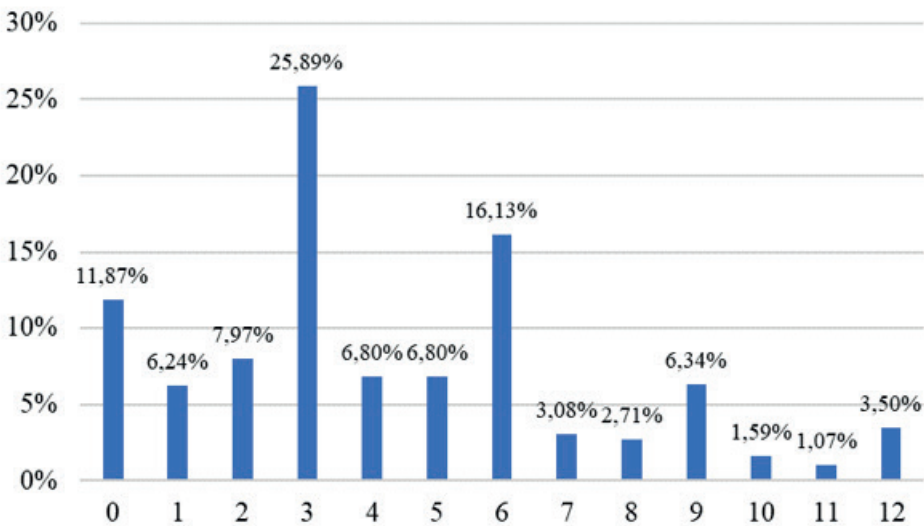

Figure 29: Monthly distribution of ventilation index values in 2018 for the Racibórz area. Vertically - share situation.

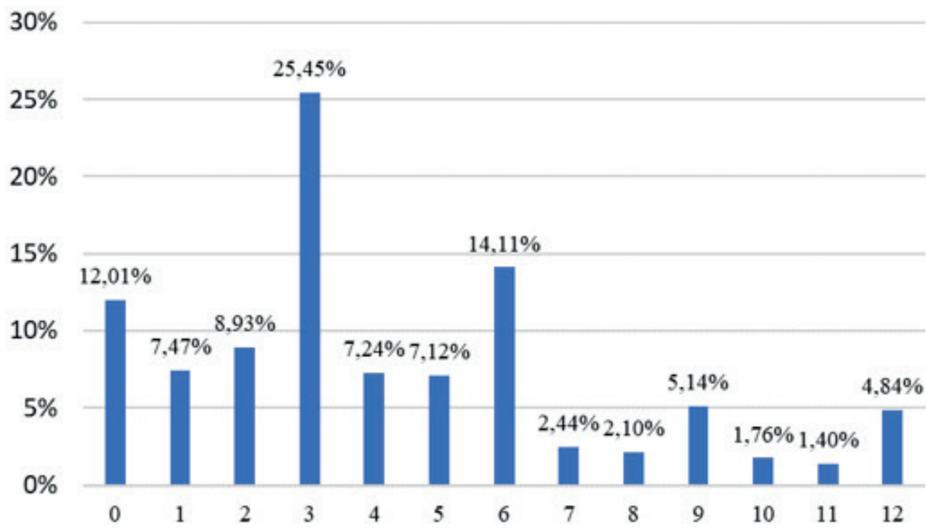

Figure 30: Monthly distribution of ventilation index values in 2018 for the Racibórz area. Vertically - share situation.

Analysis of the frequency of occurrence of the index of flow (IWW) indicates that in both years, days with good and slightly unfavourable dispersion conditions were dominated by VI < 6. Situations with unfavourable and very poor dispersion conditions occurred less than 20% of the time per year. This means that for this time of the year, smog situations on both sides of the border correspond to particulate matter emissions from sources near the ground or from roads and the ground surface.

In the light of the dispersion conditions thus formed, the wind rose chart from Racibórz looks as in Figure 31.

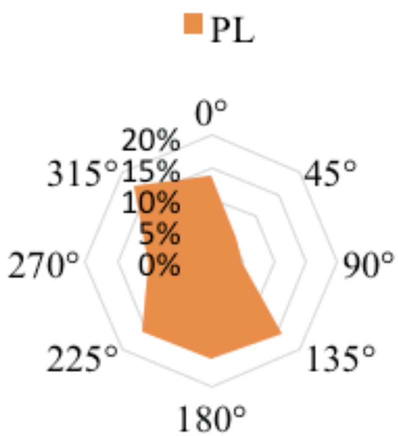

Figure 31: Wind rose chart for Racibórz for the period 2018-2019

The 2018-2019 wind rose chart is almost identical in shape to the multi-year wind rose. There is also a strong influence of landform on the prevailing wind directions.

5.4 Comparison of wind conditions and PM_{10} concentrations during joint measurements

The analysis of the results of wind direction and wind speed measurements at the measurement stations in Racibórz and Horní Suchá during the joint measurements (2018-2019) showed the similarity of the rose charts with the long-term average wind rose chart from the meteorological station in Racibórz. At both locations, the shape of the wind rose chart is influenced by general circulation processes determined by the terrain profile. In the case of Horní Suchá, a slight increase in the share of the southern direction is observed at the expense of the northwest, which may be caused by the difference in the height of the measurement and the degree of horizon coverage. The measuring station located at the foot of the tower does not provide fully representative wind direction measurement results. For the heating season (October-March), wind roses for both stations takes a more even shape, with the NE sector slightly dominant in the Horní Suchá, and the southern sector in Racibórz (Figure 32 to Figure 34). For the summer season (April-September), both roses have a similar shape to all-year roses.

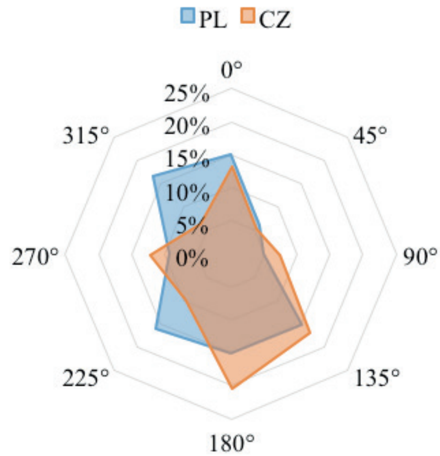

Figure 32: Wind rose chart for Racibórz (PL) and Horní Suchá (CZ) for the period 2018-2020.

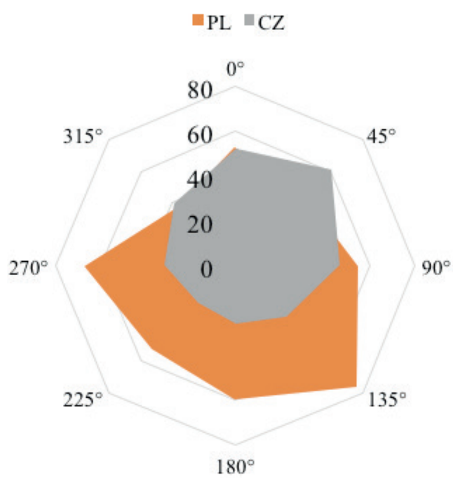

Figure 33: Wind rose chart [%] for Racibórz (PL) and Horní Suchá (CZ) for the period 2018-2019 (heating season).

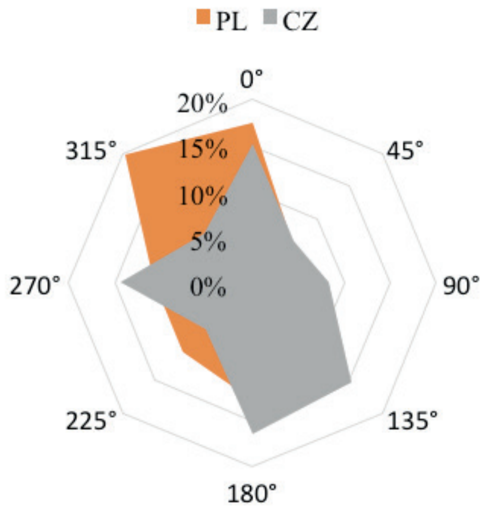

Figure 34: Wind rose chart [%] for Racibórz (PL) and Horní Suchá (CZ) for the period 2018-2019 (non-heating season).

PM_{10} concentration rose charts have an interesting shape. In all cases (year, heating season and non-heating season), the highest concentration is observed at the station in Racibórz from the south (135-225°) and in the case of Horní Suchá the influx is equal from both directions. See Figure 35 to Figure 37. This situation may be influenced by the different geographical location of the two stations, as well as by the significant difference in the height of the wind and pollution measurements.

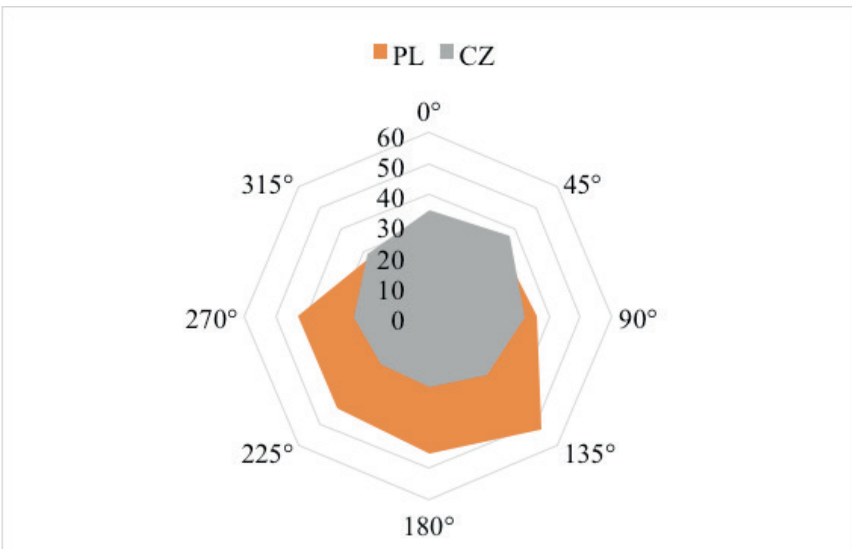

Figure 35: PM_{10} concentration rose charts [g/m^3] for Racibórz (PL) and Horní Suchá (CZ) from 2018-2019.

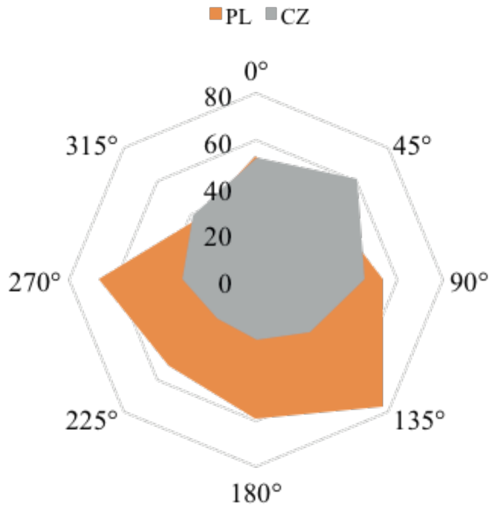

Figure 36: PM_{10} concentration rose charts [g/m^3] for Ratiboř (PL) and Horní Suchá (CZ) from 2018-2019 (heating season).

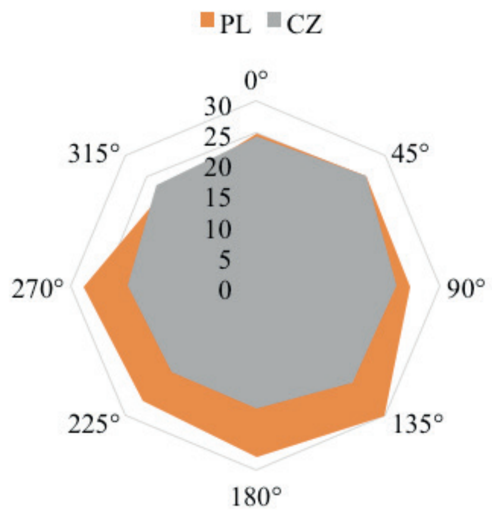

Figure 37: PM_{10} concentration rose chart [g/m^3] for Ratiboř (PL) and Horní Suchá (CZ) from 2018-2019 (non-heating season).

5.5 Summary of the meteorological research

The results of the Polish research presented in the monograph concern mainly the meteorological aspects of the transport of transboundary pollution. Thanks to the use of a radiometer - a device for measuring the vertical temperature profile in the atmospheric - the classification of thermal stratification of the atmosphere was worked out and related to the air quality. It has been shown that poor ventilation conditions are responsible for the highest concentrations of diverse PM fractions. In such situations, episodes of high pollution develop, which - although of regional importance (Ziemiański and Oródka 2012; Degórska et al. 2016) - effect equally areas located on both sides of the border. Fortunately, the meteorological situation during the research period in 2018-2020 was not conducive to frequent occurrences of smog episodes; however, the few that occurred, confirmed the thesis above. An important conclusion resulting from the research is also the fact that there are situations (up to 10% of the time a year), during which the near-surface wind vector (under inversion) was inconsistent with the upper wind (above inversion), even by 180°. This conclusion is particularly important for researchers who model pollutant transport using large-scale models, for which such situations are undetectable. This statement also has an important practical aspect: the quantitative balance of pollutants on both sides of the border should be assessed taking into account the entire profile of the atmospheric boundary layer.

6 POLLUTION TRANSFER VECTOR

The calculation of the value and direction of the pollution transfer vector is based on the measurements carried out within the AIR BORDER project and on the other hand on all other available data measured by IMGW-PIB (PL) stations on the Polish side of the area of interest and by the Czech meteorological institute on the Czech side of the area. The data from continuous measurements of meteorological parameters are analysed and the evaluated vector is represented as the value and direction of the transboundary transfer of PM_{10} via a web interface (see Figure 38) and a mobile phone application.

Figure 38: Display of project output on the website

6.1 Wind direction vector on the background of the atmosphere thermal stratification

A dynamic system for visualizing the direction of air pollution transfer (changing every hour) was designed to display the air pollution transfer. Its assumption is to simultaneously take into account the height of the inversion layer determined on the basis of radiometric data from Racibórz and the verified vertical profile of air temperature at CHMI ground meteorological stations (Lysá hora, Červená). It also includes the wind vector at 10 m above the ground in Racibórz and 80 m above the ground in Horní Suchá and pollution concentrations at air quality monitoring stations in Poland (PMŚ/GIOŚ) and the Czech Republic (CHMI).

Figure 39 to Figure 42 below show the occurrence of different situations of airborne particle transfer in the lower part of the atmospheric boundary layer. This results from the differentiation of thermodynamic conditions in this part of the atmosphere. In about 90% of the cases, the wind direction vector was similar, although not identical, at both altitudes. In about 10% of cases the wind vector direction was opposite at 10 m in Racibórz and at 80 m in Horní Suchá. The 10% of cases resulted from the location of the upper boundary of the inversion at a height lower than 85 m. This may mean that air with pollution originating from low municipal sources (local heating) dominated in the lower layer and in the layers above the inversion, there was the airflow associated with industrial emissions.

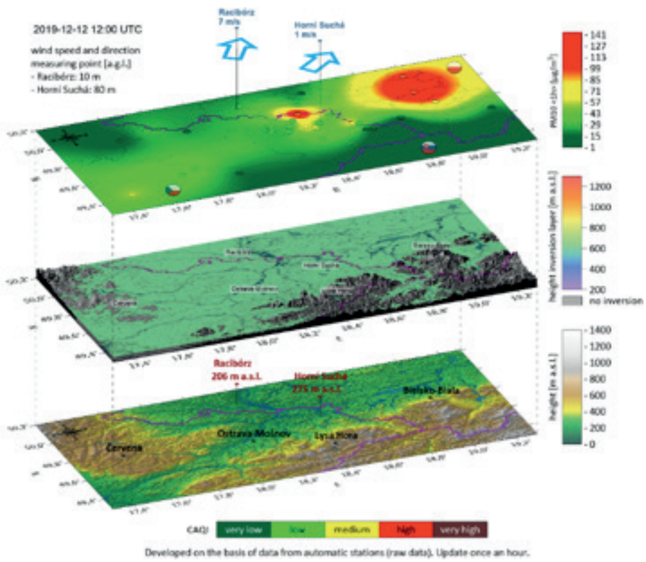

Figure 39: Case of visualization of inversion and wind vectors similar for Racibórz and Horní Suchá. Flow from CZ to PL.

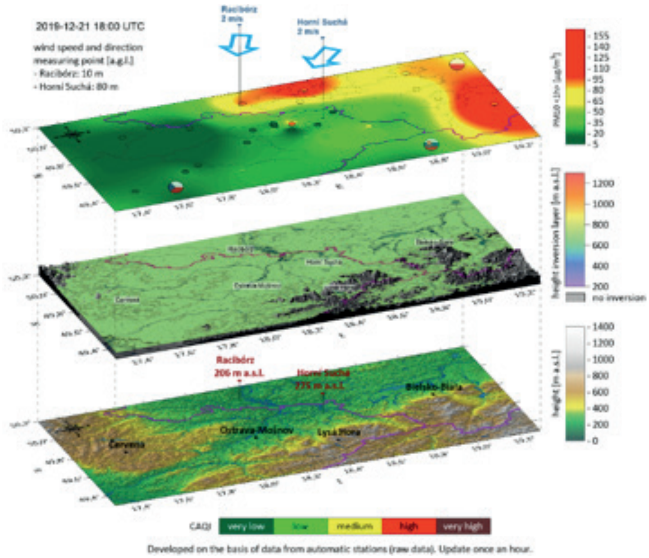

Figure 40: Case of visualization of inversion and wind vectors similar for Racibórz and Horní Suchá. Flow from PL to CZ.

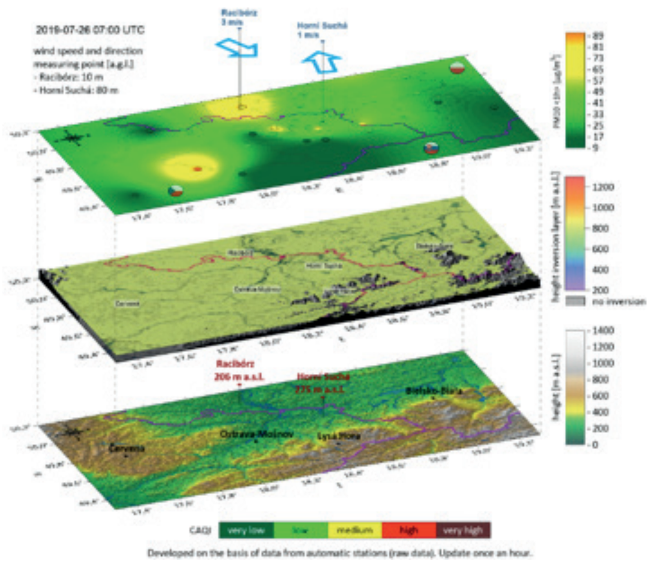

Figure 41: Case of visualization of inversion and wind vectors in the opposite direction for Racibórz and Horní Suchá. Racibórz flow from PL, Horní Suchá flow from CZ.

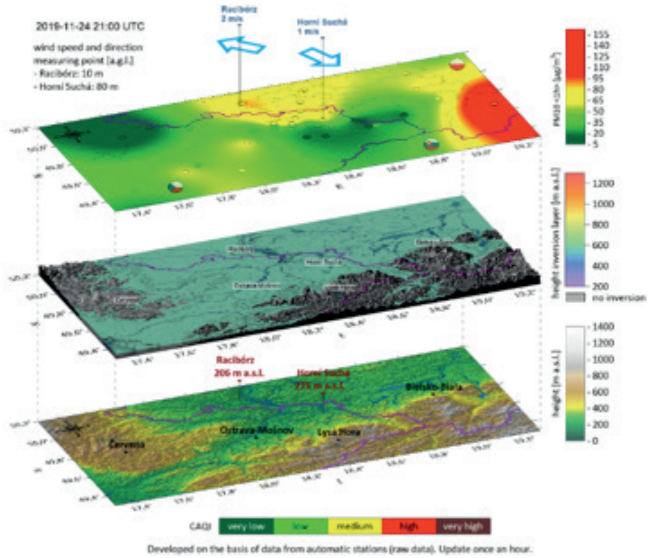

Figure 42: Case of visualization of inversion and wind vector in opposite direction for Racibórz and Horní Sucha. Ratibórz flow from CZ, Horní Suchá flow from PL.

6.2 Analysis of the situation with high pollution concentrations

On 19 December 2019, a situation with extremely high concentrations of suspended PM occurred. This situation has been analysed in detail separately.

The synoptic map in Figure 43 shows that southern Poland was under the influence of a large pressure high centred over the Balkan in a warm polar-marine air mass. A southwestward flow of air masses was observed over the inversion layer. A low temperature inversion occurred at night and mid- and low-level stratocumulus cloud piles were maintained. The average daily temperature was 6.3°C. The lowest temperatures of around -0.4 °C occurred at night and in the evening.

In the morning hours, the opposite wind vector direction was observed in the layer below the inversion. There was a light wind from the northeast. It is possible that pollution flowed in this layer from the Polish area to the Czech Republic. In the layer above the inversion, an inflow of air from the south was observed. See Figure 44 (a). In the afternoon, both wind vectors (the lower one in Ratibórz and the upper one in Horní Suchá) came from the south. See Figure 44 (b).

The highest recorded concentrations of PM_{10} and $PM_{2.5}$ were observed during the night hours when there was a significant layer of ground-level inversion (with a maximum thickness of 250 m above the surface) for the time duration of 11 h (from 01:00 to 12:00 UTC). During this time, the ceilometer recorded a layer of height inversion occurring about 1 000 m above the ground during the night hours and then from 12 h to midnight. The highest concentrations of suspended PM were recorded around 16 h UTC and were likely related to the release of pollution from the inversion layer into the entire mixing layer profile. See Figure 45.

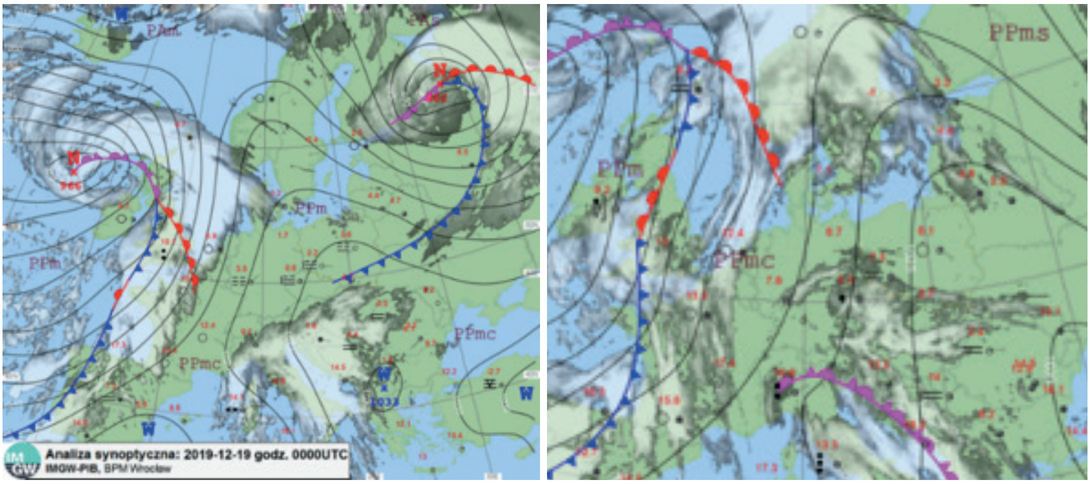

(a) (b)

Figure 43: Synoptic situation map from 19 December 2019; time 0:00 UTC (a); 12:00 UTC (b) (source: IMGW-PIB).

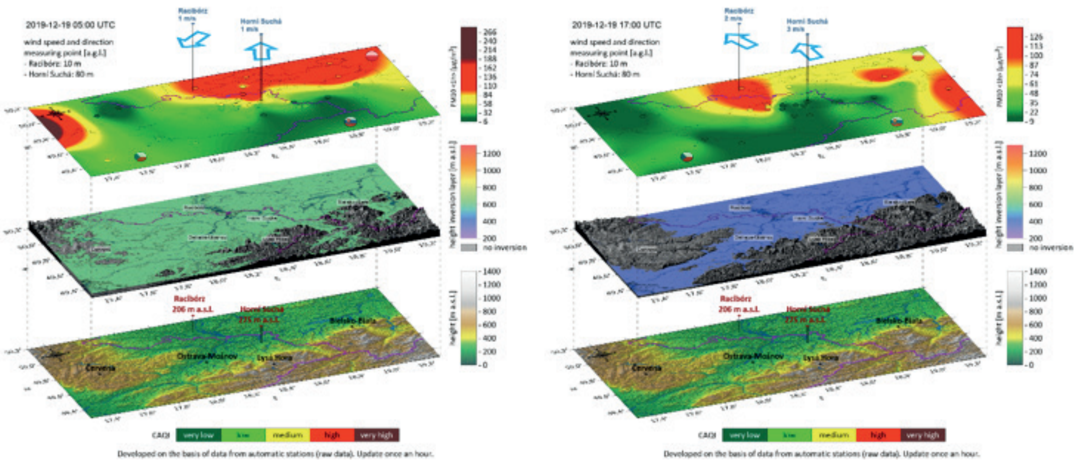

(a) (b)

Figure 44: Visualization of inversion and wind vector at high concentrations of PM_{10} and $PM_{2.5}$ on 19 December 2019 - situation in the morning 5:00 UTC (a); situation in the evening 17:00 UTC (b)).

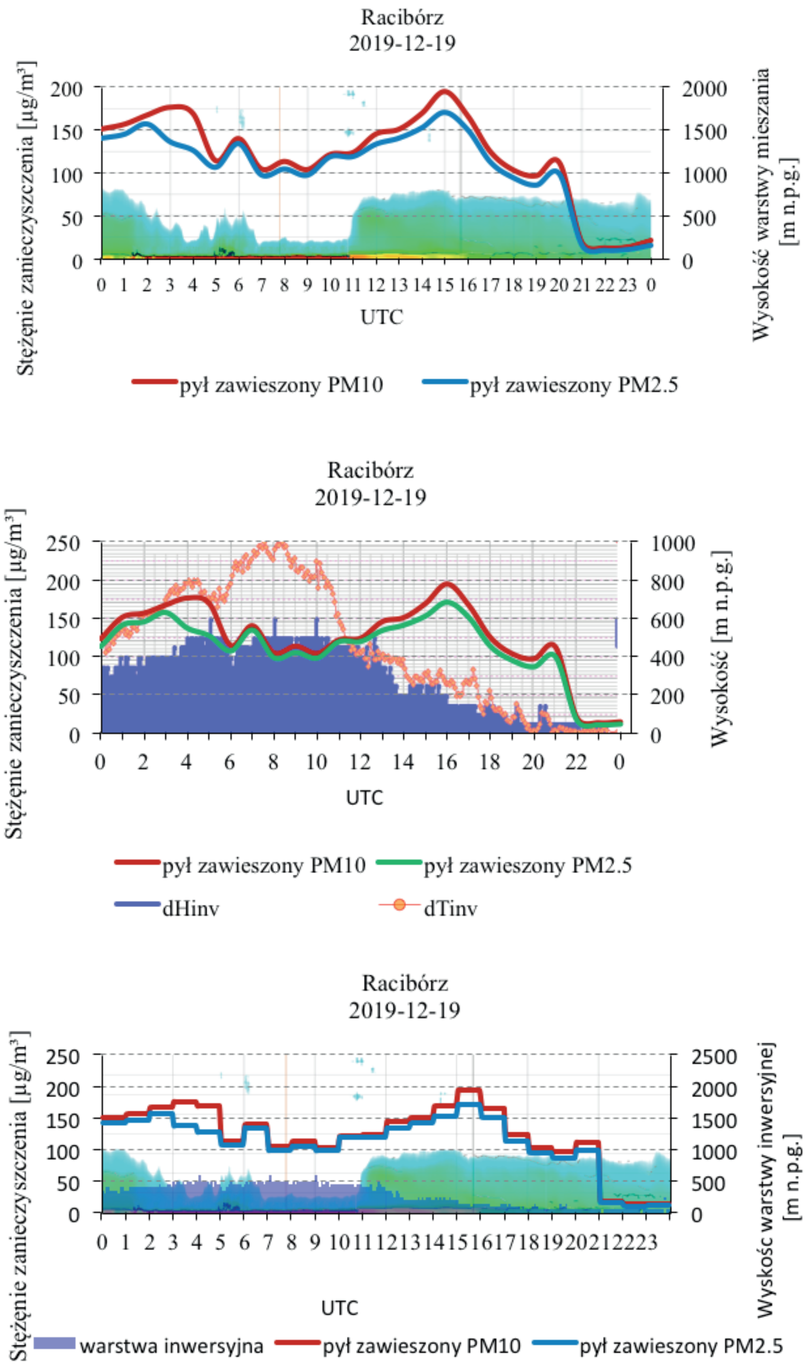

Figure 45: Visualisation of PM_{10} and $PM_{2.5}$ concentrations on 19 December 2019 using radiometer and ceilometer (dHinw - height of the mixing layer, dTinw - height of the temperature inversion). Ratibórz, vertical: pollution concentration / height of the mixing layer (m AGL)

7 EVALUATION OF SUSPENDED PARTICULATE MATTER MONITORING IN HORNÍ SUCHÁ

At the monitoring site in Horní Suchá, suspended PM particles were monitored continuously (at the base and the top of the tower) and at the same time, PM_{10} particles were sampled to determine the elemental composition and subsequent analyses of the origin of the sampled particles.

7.1.1 Pollution directional dependence analysis

The horizontal dispersion of emissions is influenced by wind speed and direction. Higher flow velocities generally lead to faster dilution and thus to lower concentrations of air pollutants. Stronger winds also lead to the development of mechanical turbulence and thus contribute to vertical mixing of the atmosphere (Kurfürst 2008).

At the measurement site on the tower, the predominant flow axis is southwest-northeast, which corresponds to the prevailing regional wind directions in the area of the Czech-Polish border (Blažek 2013; Czech Hydrometeorological Institute 2019), but the measured flow velocities are significantly higher. This is also evident in comparison with the measurements at the base of the tower, where wind speeds are up to 6 $m.s^{-1}$ (see Figure 46). It is also apparent from the wind rose charts that the measurements at the base of the tower are likely to be shielded from the north by the buildings present, or by the tower itself from the east, and it is necessary to take this into account when interpreting the results.

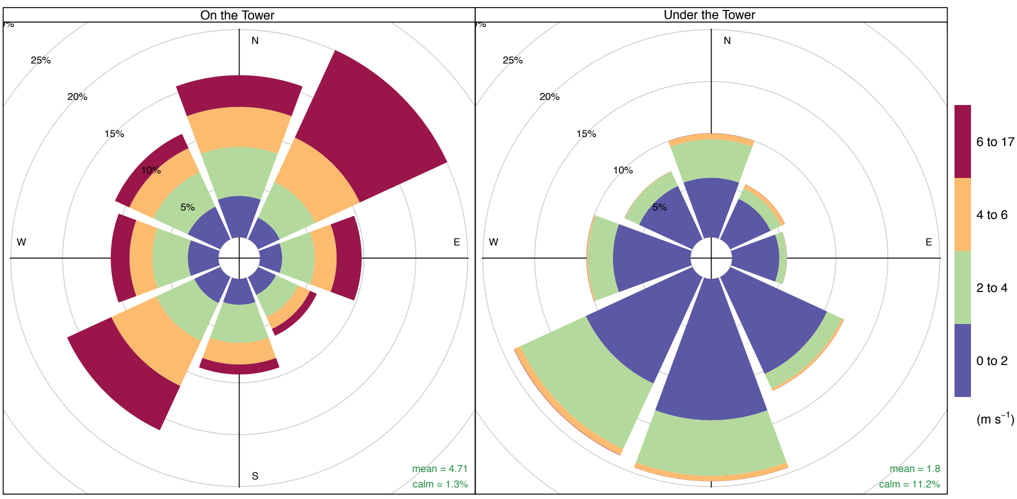

Figure 46: Velocity-distributed wind rose charts on the tower (left) and at the base of the tower (right) for the period 3/2019 - 2/2020

If we differ the wind speed rose charts by season, we can see a significant difference in the prevailing wind direction at the top and the base of the tower during the cold season, see Figure 47. While the prevailing direction at the tower top is clearly NE, followed by a northerly flow, at the base of the tower the prevailing flow direction is exactly the opposite, i.e. southwest and south.

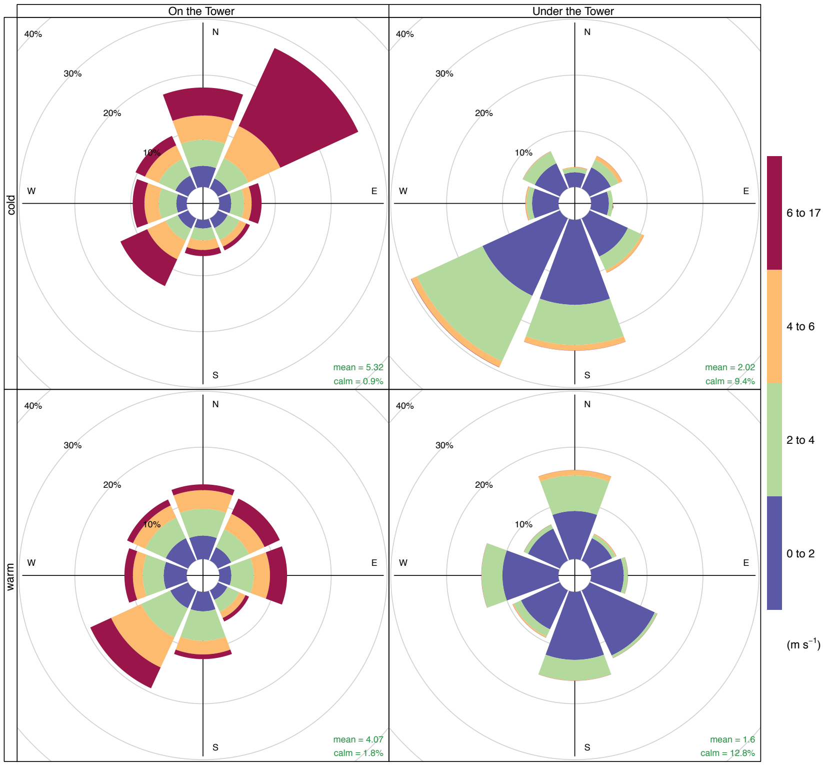

Figure 47: Velocity-distributed wind rose charts on the tower (left) and at the base of the tower (right) and in the cold season (top) and warm season (bottom) for measurements 3/2019 - 2/2020

The effect of wind speed and wind direction on the determined pollutant concentrations can be expressed by the so-called weighed concentration rose chart, see Figure 48. From the data processed in this way it can be seen that situations with south-easterly, southerly and south-westerly flow at wind speeds up to 2 m.s^{-1} contributed most to the average PM concentrations at the base of the tower. The influence of the adjacent service road is evident here, which during the period under assessment was mainly used by lorries travelling to the ongoing construction of the hall in the western part of the industrial zone.

It is also evident from the weighed concentration rose charts in Figure 48 that the contributions from each direction to the average PM concentrations at the tower are relatively evenly distributed, with more significant transfer in the most southwesterly and northeasterly flow directions. Higher contributions are evident for all PM fractions in the 7-8 m.s^{-1} flow speed range from the northeasterly direction, with this effect becoming more emphasized during the cold part of the year (heating season). This probably indicates the presence of a more distant energy source in this direction.

A comparison of the weighed concentration rose charts at the tower and at the base of the tower also shows a clear difference in the contributions at individual wind speeds, with significant contributions at flows up to 4 m.s^{-1} below the tower, whereas at the tower up to 10 m.s^{-1}. When comparing the individual PM fractions, the differences are then minimal.

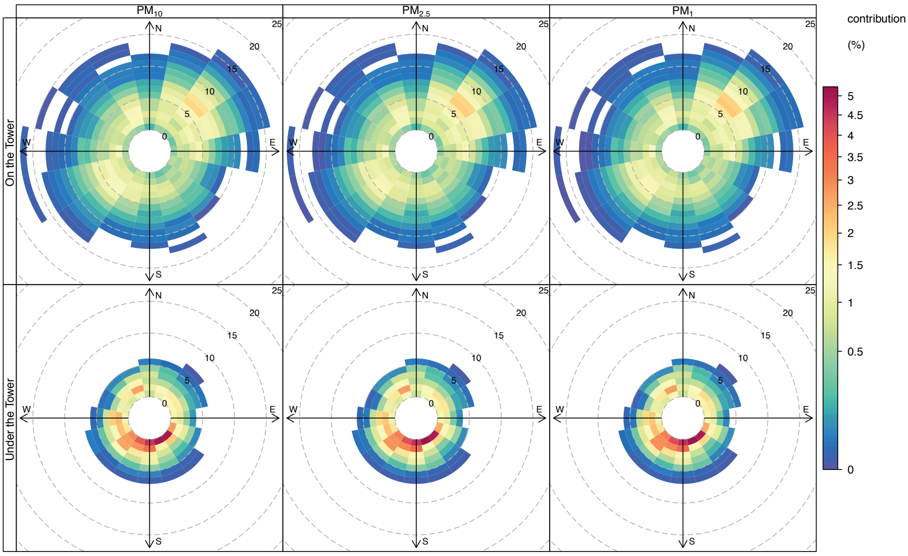

Figure 48: Weighted concentration rose for PM_{10} (left), $PM_{2.5}$ (centre) and PM_1 (right) at the tower (top) and at the base of the tower (bottom)

If we consider only the direction from which the pollution came, we get contributions by wind direction (see Figure 49). These contributions have been divided by season - into the warm (non-heating) season: April-August (Figure 49 (a)), and the cold (heating) season: September-March (Figure 49 (b)). From the rose charts weighed in this way, the difference in the directionality of the contributions between seasons and between the locations of the measuring devices is visually clear. To clarify the interpretation, it should be emphasized that in this case it is a representation of the proportion, not the absolute amount of concentrations from a given direction.

During the summer period, contributions at the base of the tower are most significant from the south and southeast (from the direction of the service road), with higher contributions also recorded from the west where construction activity was in progress. In winter, the most significant contributions at the base of the tower are from the south to south-west, indicating the influence of local heating from the adjacent Horní and Prostřední Suchá municipalities respectively. Differences between the individual fractions are not visible.

On the top of the tower, the contribution from the north-east dominates in the summer. This may be the influence of mining activity (see Figure 7). In the winter period, the tower top is dominated by the contribution from the east-northeast, probably a source related to heating or long-distance transfer from Poland, as the influence is higher for the smaller particle fractions.

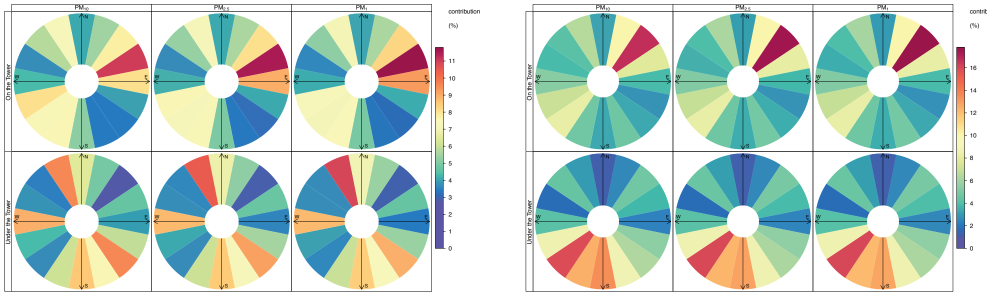

(a) (b)

Figure 49: Directionally-weighted concentration rose charts for warm (a) and cold season (b) - PM_{10} (left in figures), $PM_{2.5}$ (centre in figures) and PM_1 (right in figures) at the towertop (top in figures) and at the base of the tower (bottom in figures)

The concentration rose chart divided by season (Figure 50) shows that the highest short-term average PM concentrations arrive at the tower in winter in the direction of the prevailing winds, i.e. from the northeast and southwest, and at low flow velocities of about 5 $m.s^{-1}$. In the warm season, the towertop is affected by sources from the northeast and east (probably mining activities) and southwest (probably the metallurgical plant in Třinec), see. Figure 7. At the base of the tower, concentrations are higher at flow velocities up to 1 $m.s^{-1}$, and in summer the influence of construction activity sources around the north-west is evident at higher flow velocities, around 6 $m.s^{-1}$

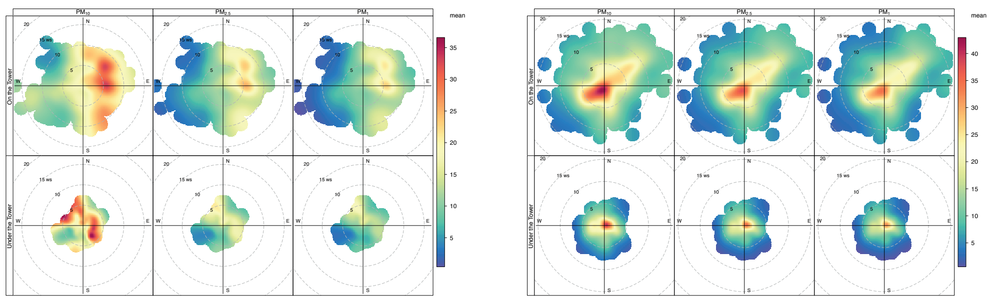

(a) (b)

Figure 50: Concentration rose charts for warm (a) and cold season (b) - PM_{10} (left in the figures), $PM_{2.5}$ (centre in the figures) and PM_1 (right in the figures) at the towertop (top in the figures) and at the base of the tower (bottom in the figures)

7.1.2 Pollution time course analysis

As expected, measured PM concentrations show a significant annual variation with highest concentrations during the heating season (Figure 51 and Figure 52). Conversely, the lowest concentrations were recorded during summer. Generally, higher concentrations were measured at the station at the base of the tower during the winter season than at the station at the towertop. Thus, it can be assumed that the local heating is the most important contributor to the increase in concentrations during the winter season, which also corresponds to the differences in concentrations between years. The station at the base of the tower is probably influenced by local heating from nearby villages (Horní and Prostřední Suchá), while the station on the towertop is influenced by long-distance transmission from

Poland (see also Figure 48). Figure 52 also shows the occurrence of several peak concentrations at the station at the base of the tower in April and November 2018 and November 2019, respectively. These were due to dusty construction works that took place in the vicinity of the station in the months concerned.

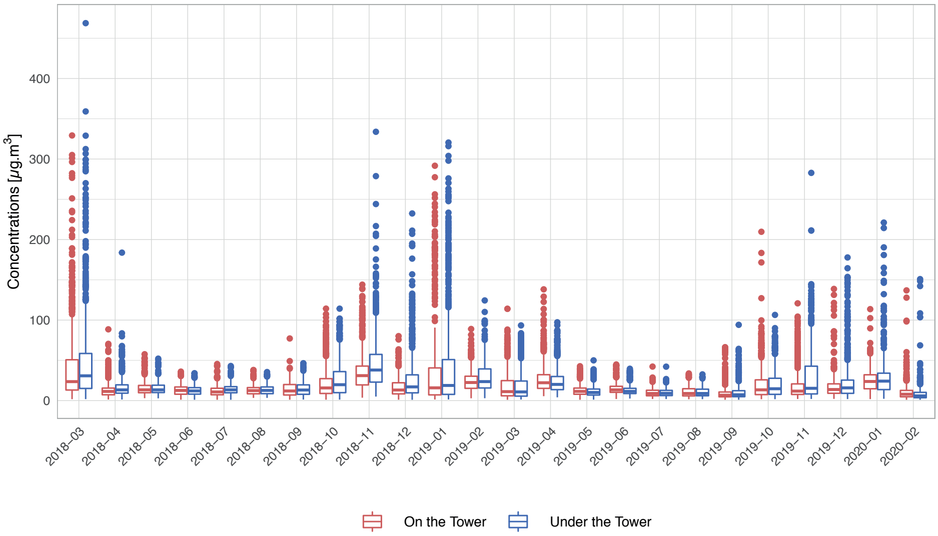

Figure 51: Monthly variability of daily $PM_{2.5}$ concentrations at the towertop and at the base of the tower

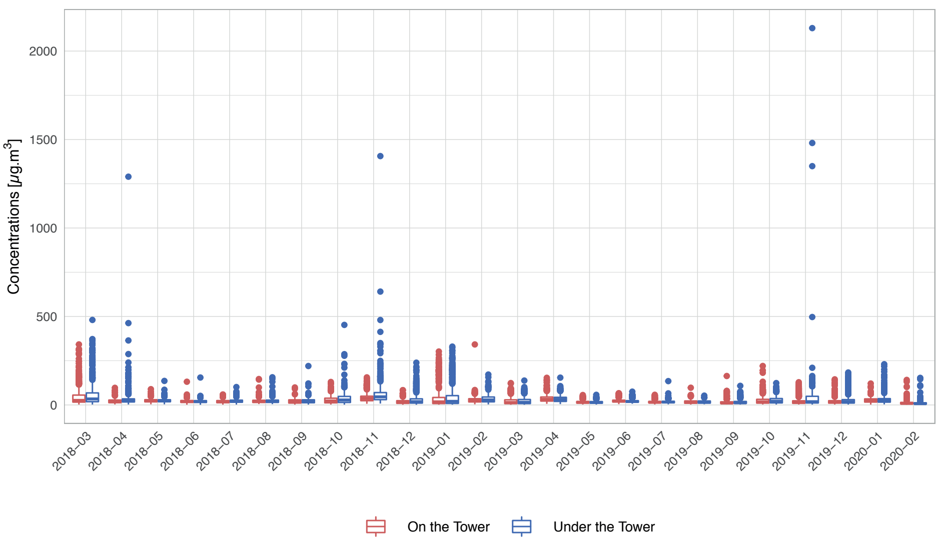

Figure 52: Monthly variability of daily PM_{10} concentrations at the towertop and at the base of the tower

Daily PM concentrations also show some variability within the weekly pattern - see Figure 53 and Figure 54. This is again evident within the cold winter period and is probably related to heating. Particularly in winter 2019, an increase in concentrations at weekends can be noticed (especially on Saturdays at the station at the base of the tower), but this trend is not evident in winter 2020. PM concentrations measured in the summer period do not show a weekly pattern.

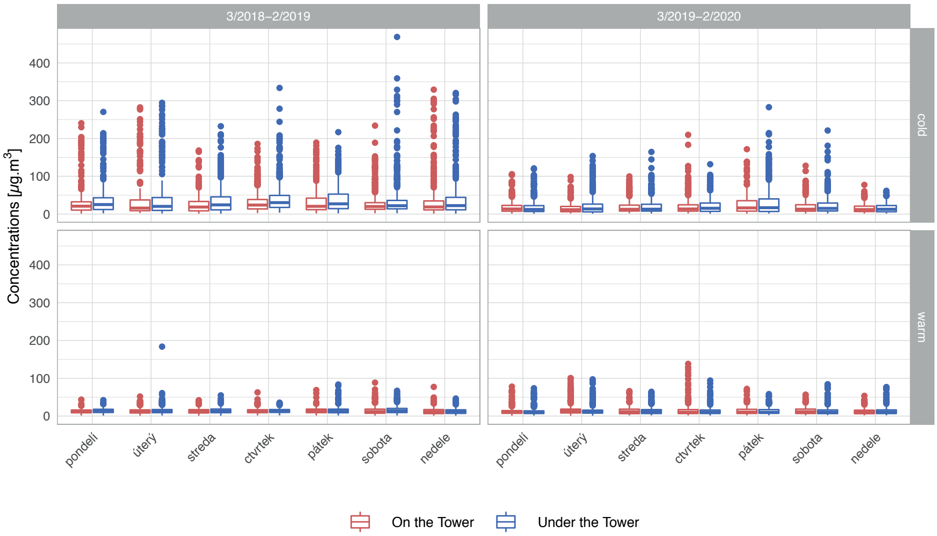

Figure 53: Weekly variability of daily $PM_{2.5}$ concentrations at the towertop and at the base of the tower

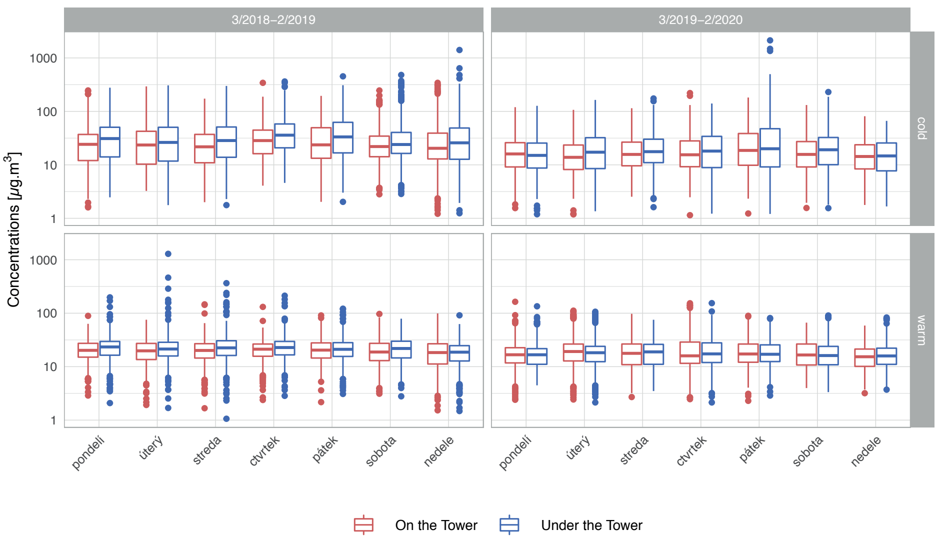

Figure 54: Weekly variability of daily PM_{10} concentrations at the towertop and at the base of the tower

7.1.3 Evaluation of measurements

Within this activity, concentrations of suspended particulate matter fractions PM_1, $PM_{2.5}$, PM_{10} and total suspended particles (TSP) were continuously measured. In addition, basic meteorological variables such as temperature, pressure, humidity, wind speed and direction were also monitored. Based on the analyses performed, it can be concluded that the measured PM concentrations at the station at the base of the tower are generally higher than at the station at the towertop, with the difference being more significant, as expected, for the larger particles (PM_{10} fraction and larger) and during the winter season. At the tower base station, the measurements are influenced by local pollution sources such as local heating, traffic from the adjacent service road or construction activities in the industrial zone. The station at the towertop is then influenced more by long-range transmission.

From the recorded wind speed and direction at the towertop station, it can be seen that in winter the prevailing flow is from the north-east and north, i.e. from Poland, and the concentrations at the tower are thus influenced by transboundary transfer of pollution. In summer, on the other hand, south-westerly flow prevails at the tower. From the recorded temperatures, it is possible to determine the extent and frequency of temperature inversions and the dependence of suspended particulate matter concentrations on the temperature difference. Long-term continuous observations of meteorological variables at this non-standard height of about 90 m above the ground may subsequently help to better understand the processes of pollution transfer in the region.

The observations of wind direction and wind speed at the station below the tower should be interpreted taking into account the fact that the measurements were influenced by the surrounding buildings, especially the tower itself (from the eastern direction). However, from the point of view of measuring pollution and providing the infrastructure necessary for the operation of the station, this was the most suitable location.

When comparing the determined annual concentrations of PM_{10} and $PM_{2.5}$ for the monitored period (3/2018 - 2/2019 and 3/2019 - 2/2020) with the annual limit values for these pollutants (European Council 2008), it can be stated that in the case of PM_{10} the limit of 40 µg.m^{-3} was respected, in the case of $PM_{2.5}$ the limit of 20 µg.m^{-3} was exceeded (except for the value determined for the period 3/2019 - 2/2020 at the towertop station). See Figure 55 and Figure 56. However, it should be taken into account that these are annual concentrations determined for the observation period, not for a calendar year set by the legislation. It can be seen from Figure 55 and Figure 56 that the measured PM concentrations are consistent with those measured in the region in concerned years. The most similar values were determined at the CHMI station in Havířov, which is also the closest station to the base of the tower. The towertop station generally shows lower pollution values.

The year-on-year comparison shows a decrease in suspended particulate matter concentrations both at the stations in František and in the whole region. According to the Czech Hydrometeorological Institute, the annual average concentrations of PM_{10} and $PM_{2.5}$ in 2019 were the lowest in the past decade (Czech Hydrometeorological Institute 2020). The reason for the decrease of pollution was both the good dispersion conditions of the year and the general decline of emissions in the region.

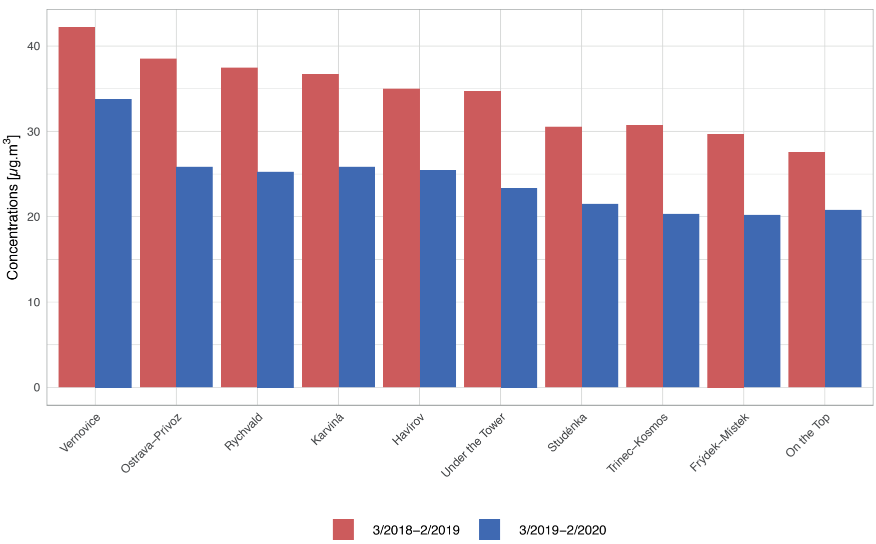

Figure 55: Comparison of average PM_{10} concentrations determined at the towertop and at the base of the tower over the observation period with annual average PM_{10} concentrations at other stations in the region

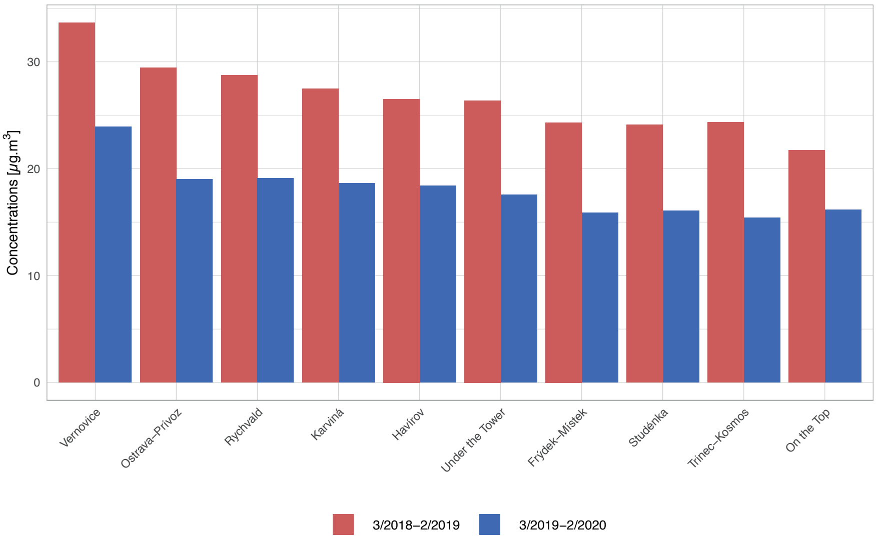

Figure 56: Comparison of average $PM_{2.5}$ concentrations determined at the towertop and at the base of the tower over the observation period with annual average $PM_{2.5}$ concentrations at stations in the region

7.2 Sampling of suspended particles on filters

Using the equipment described in Section 4.2.2, 111 samples of PM_{10} were collected on filters and analysed within the project implementation. Samples were collected from 8 basic wind directions and during calm, 3 samples were collected during smog situations. The filters were exposed to pollution for one month each time between April 2018 and March 2019, for a total of 12 months. The evaluation of the measurements is based on a scientific paper (Pavlíková et al. 2020).

7.2.1 PM_{10} concentration

PM_{10} mass concentrations were determined in accordance with EN 12341 (European Committee for Standardization 2014). The filters were weighed on analytical balances (Sartorius MC 210P) before and after sampling. Prior to weighing, filters were tempered for ≥ 48 h at a controlled relative humidity (50% ± 5%) and temperature (20 °C ± 1 °C), then weighed for the first time, and after a further tempering for ≥ 12 h followed a second weighing. After sampling, the filters were weighed after 24 to 72 h. As required by the standard, a difference in weighing results of ≤ 40 µg for the filters before sampling and ≤ 60 µg for the filters after sampling was maintained. The filter weight was calculated as the average of the two measurements. Blank filters weights were also recorded. The PM_{10} deposition was calculated by subtracting the pre-exposure weight from the post-exposure weight of the filters.

The values of PM_{10} concentrations corresponding to wind directions, calm and inversion situations are given in Table 4 as an annual average, average for the warm period (April to September) and average for the cold period (October to March) for observations from April 2018 to March 2019.

Table 4: Average PM_{10} concentrations for the period in question ($\mu g.m^{-3}$).

Wind conditions	**Average** [1]	**Average warm period**	**Z-score** [2]	**Average cold period** [1]	**Z- score** [2]
Calm	23,3	19,0	-0,35	27,6	1,16
N	22,9	14,6	-1,12	31,2	1,79
NE	21,7	16,5	-0,79	27,0	1,05
E	25,0	17,8	-0,56	32,3	1,97
SE	21,1	17,5	-0,60	24,6	0,64
S	21,9	16,9	-0,71	27,0	1,05
SW	14,8	14,5	-1,14	15,1	-1,04
W	21,3	23,6	0,45	19,0	-0,35
NW	16,8	15,9	-0,89	17,8	-0,56

[1] *Averages calculated for the period in question (04/2018-03/2019), inversion concentrations not included.*

[2] *Z-score of average values calculated for the period in question (04/2018-03/2019).*

7.2.2 PM_{10} origin determination

The lowest PM_{10} values were observed from the SW and NW direction regardless of the season. Concentrations were below average in the warm part of the year, except in the west direction due to the high concentration in August 2018 (Figure 57). The highest concentrations were sampled from the east and north in the cold season, although the prevailing wind direction was SW, see Figure 57 (b). The prevailing wind direction during the cold season was also the prevailing wind direction for the entire observation period, as shown in Figure 57 (b) (expressed as volume of air sampled). Calm was recorded for 12% of the sampling time.

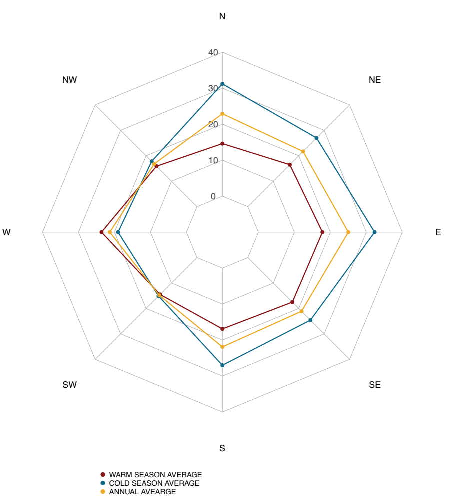

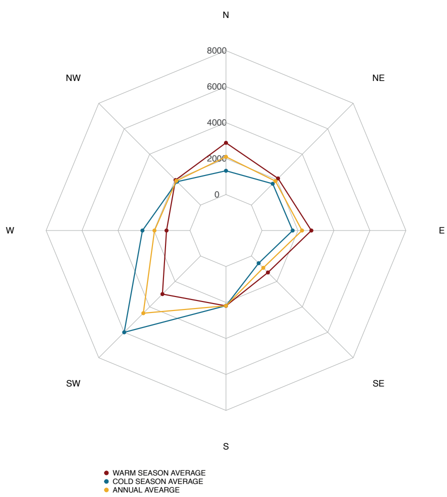

(a) *(b)*

Figure 57: Average PM_{10} concentrations (a) and wind rose charts over the period of interest (b).

Apart from the peak concentration observed in August 2018, no significant directionality of pollution is evident in the warm season. See Figure 58 (a). The peak August concentration most likely originated from the metallurgical complex west of the monitoring station (see Figure 7), as suggested by the elemental composition of this sample. According to meteorological data, this high concentration occurred during a period of steady cyclonic airflow (wind speed from calm to 2 m.s^{-1}) preceding an approaching cold front.

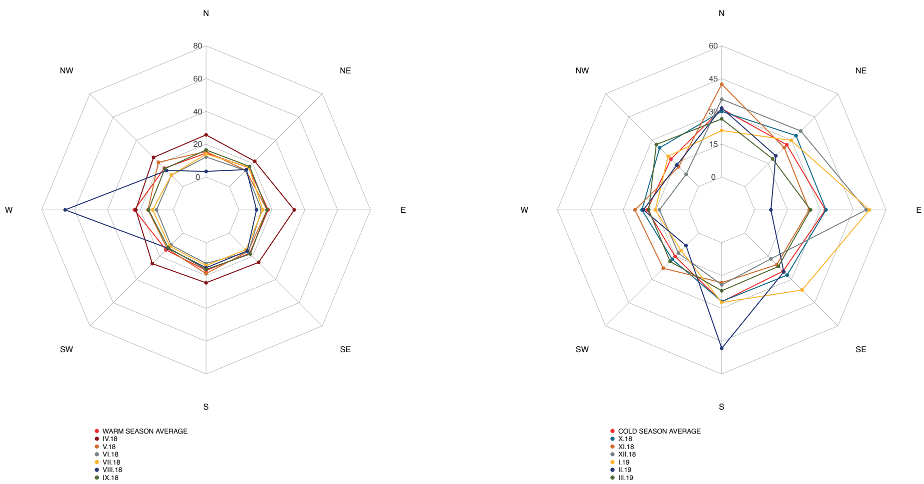

(a) (b)

Figure 58: Average monthly PM_{10} concentrations for warm (a) and cold (b) periods.

The April concentration rose has a similar pattern to that of March (Figure 58). With respect to the elements found in the samples, a similar origin of pollution can be assumed. Thus, April PM_{10} concentrations are more likely to be related to cold season pollution sources.

Pollution in the winter period came mainly from the north, northeast and east, as shown by the monthly average PM_{10} concentrations in Figure 58 (b). This confirms the importance of PM transfer from the Polish border area. The increase in PM_{10} concentrations from these directions in winter is on average 14 µg.m^{-3}, although the prevailing flow direction in winter is the opposite (Figure 57 (b)).

High concentrations of PM_{10} were also sampled from the south in February 2019 during the winter period. As there is no significant source of pollution in this direction, these concentrations were examined more closely. Meteorological data showed that the flow was stable (wind speed 1-2 m.s^{-1}), coming through the Moravian Gate from the southwest, accompanied by a radiative inversion (see Figure 59). This suggests that the peak concentration was coming from a significant pollution source in the southern part of the Moravian Gate. This was probably a cement factory near Hranice na Moravě (about 50 km from the sampling site), as also suggested by the elemental composition of this sample.

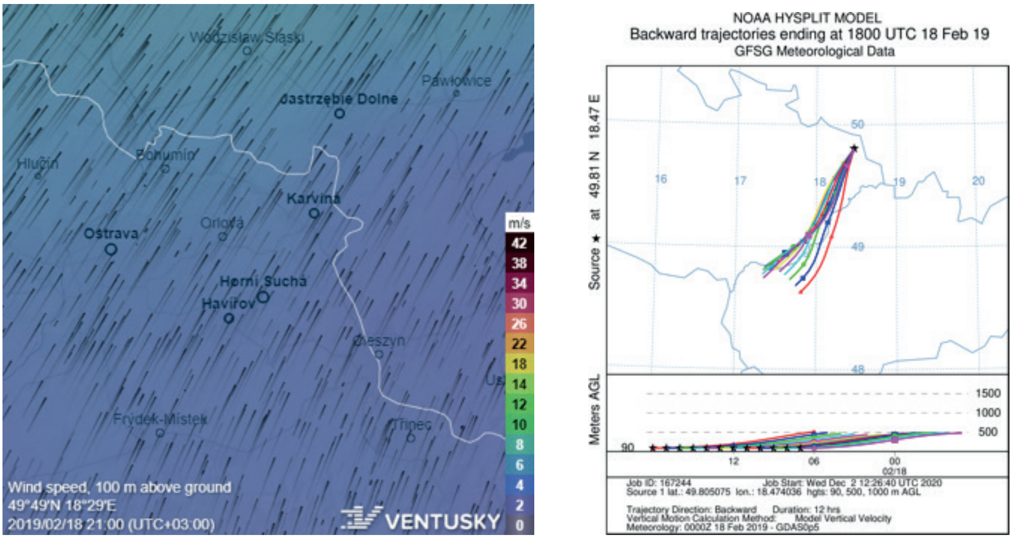

(a) (b)

Figure 59: Modelled wind field (a) and backward trajectories (b) for the peak concentration in February 2019 (InMeteo 2020; Stein et al. 2015; Rolph et al. 2017).

Samples were also collected during two smog events in the winter season, the first on 19 and 23 November 2018 (sampled on the same filter) with a PM_{10} concentration of 60.5 µg.m^{-3}, and the second on 23 March 2019 with a PM_{10} concentration of 57.4 µg.m^{-3}. In both cases, the temperature inversion was associated with a steady airflow (measured wind speed <1 m.s^{-1}). In November, the prevailing airflow was from the NE, E and SE directions. This most likely represents an influx of pollution from the metallurgical complex to the southeast of the sampling site (see Figure 7), as confirmed by backward trajectory modelling (see Figure 60). For the March smog situation, the modelled airflow shows a direction from NE and E, suggesting the origin of the pollution in the Polish border region (see Figure 61). The elemental composition of these samples is presented in the following chapter.

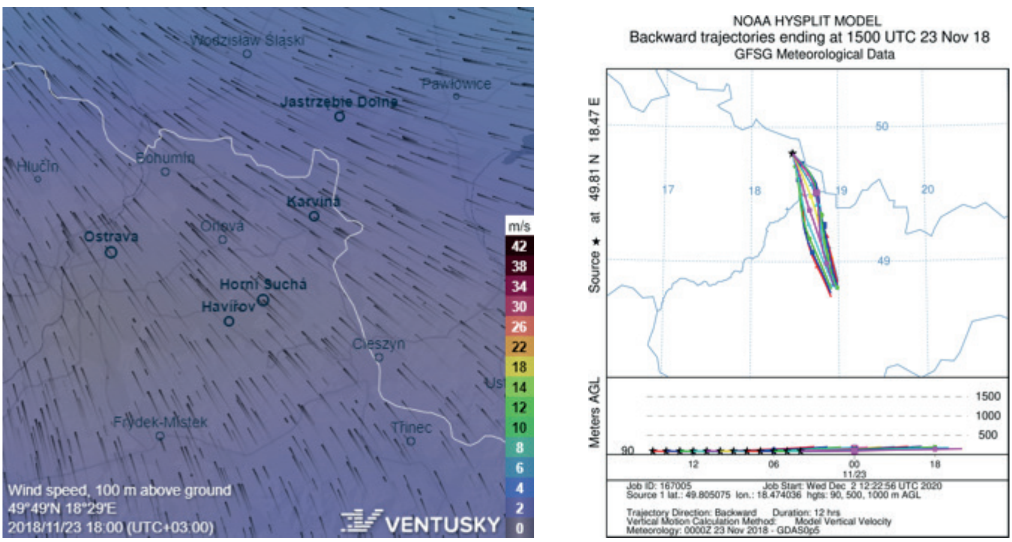

(a) (b)

Figure 60: Modelled wind field (a) and backward trajectories (b) for smog conditions in November 2018 (InMeteo 2020; Stein et al. 2015; Rolph et al. 2017)

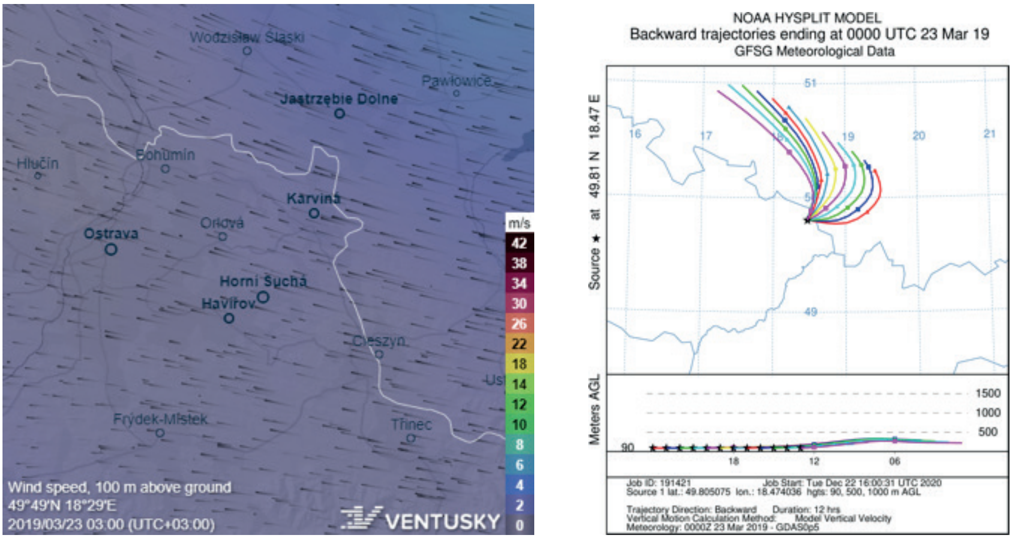

(a) *(b)*

Figure 61: Modelled wind field (a) and backward trajectories (b) for the smog situation in March 2019 (InMeteo 2020; Stein et al. 2015; Rolph et al. 2017).

7.2.3 Characterisation of elemental composition by neutron activation analysis

One of the key activities of the project was to characterise the sampled PM_{10} particles using neutron activation analysis (NAA) performed at the IBR-2 reactor of the Joint Institute for Nuclear Research (Russia).

Before subjecting the samples to NAA, subsamples of exposed and empty filters were prepared, because the capsules used for pneumatic transport of the samples for irradiation are of a limited volume (Ø 18 mm) and the entire filter does not fit into them. The preparation of subsamples also allowed multiple subsamples to be loaded into one capsule, so that samples from one month and the corresponding blank filter could be irradiated together under the same conditions. For this purpose, a special automatic punching head was designed and manufactured (materials used: stainless steel, Teflon and coated synthetic rubber). Before cutting, the filters were folded in half to prevent the loss of the sampled material. Four sets of circles (Ø 16 mm) were then cut from the folded filter using layering. In this way, one subsample of each filter (comprising eight layers of exposed filter) was prepared, reaching a weight of 0.06-0.07 g, depending on the exposure. The preparation of the filters was carried out at a relative humidity of 50% (± 5%) and a temperature of 20°C (± 1°C). After preparation, each subsample was vacuum packed for transport to NAA.

For NAA, the samples were unpacked, weighed at controlled relative humidity and temperature, and placed in polyethylene and aluminium cups for short-term and long-term irradiation, respectively. They were then placed in irradiation capsules and transported to the reactor.

Applied NAA is based on activation with epithermal neutrons at low temperatures and is therefore suitable for this type of samples. Complete information on the irradiation process, measurement and quality control can be found in other works (Frontasyeva et al. 2010; Pavlov et al. 2016).

Channel 2 (epithermal neutrons, flux density φepi= 2.0×1011 cm-2.s^{-1}) was used for short-term radiation with a radiation time of about 3 minutes. Samples were measured after a 3-5 min decay time for 15 min. The isotopes of

Al, Ca, Cl, I, Mg, Mn, Si, Ti and V were determined in this way. For long-term radiation, a Cd screened Channel 1 (epithermal neutrons, flux density φepi= 2.0×1011 cm-2.s^{-1}) with an irradiation time of approximately 4 days, was used. After a 4-day cooling period, the samples were repacked and measured twice. The first time, they were measured directly after repackaging for 30 min for the determination of As, Br, K, La, Na, Mo, Sm, U and W, and the second time 20 days after the end of irradiation for 1.5 h for the determination of Ba Ce, Co, Cr, Cs, Eu, Fe, Hf, Ni, Rb, Sb, Si, Sc, Se, Sr, Ta, Tb, Th, W, Zn and Zr.

Gamma spectra of activated samples were measured on HPGe detectors (resolution 1.9 keV for 60Co 1 332 keV line, efficiency 40%). The obtained gamma spectra were then processed using GENIE-2K software (CANBERRA) with peak fit verification in interactive mode. The elemental concentrations were calculated using certified reference materials irradiated simultaneously with the samples using the „CalcConc" software developed at the Frank Laboratory of Neutron Physics, Joint Institute for Nuclear Research (Pavlov et al. 2016). Element concentrations were calculated by deducting the corresponding blank filter values from the determined element values in the subsample and recalculating using PM_{10} mass concentrations. In the case of values below the detection limit, half of the detection limit was used. In the case of missing values (no data) due to technical issues during analysis, data imputation was used to preserve information in the dataset and allow multivariate analysis (Dray and Josse 2015). For missing data that were not below the detection limit, the k-nearest neighbours (knn) algorithm was used (Hron et al. 2010)

The NAA followed the recommendations of the US EPA (Environmental Protection Agency 1999), taking into account the standard operating procedures of the workplace. Quality control of the NAA results was ensured by the joint analysis of three different standards for each batch of samples. The following standard reference materials were used: 2709a-San Joaquin Soil Baseline Trace Element Concentrations from the National Institute of Standards and Technology (NIST), 2710a-Montana I Soil Highly Elevated Trace Element Concentrations (NIST), 2711a-Montana II Soil Moderately Elevated Trace Element Concentrations (NIST), 1632c Trace Elements in Coal (Bituminous) (NIST), 1633c Trace Elements in Coal Fly Ash (NIST), AGV-2 Andesite from the United States Geological Survey (USGS), and 433 from the Institute for Reference Materials and Measurements (IRMM). Satisfactory correspondence was achieved between the experimental results and the certified material. The accuracy expressed as a percentage deviation from the certified value was < 10%.

Although the applied analytical method allows the determination of a wide range of elements, it has its specific limitations. Therefore, some important markers that would facilitate the identification of pollution sources are missing in the obtained elemental composition. These are the concentrations of Pb (not determine), Cd, Cu, Ni and Ti (only determinable at high concentrations).

The minimum and maximum values, means and medians of the elements determined in PM_{10} are presented in Table 5; the correlations of the analysed elements are presented in Table 6.

Table 5: Summary table (minimum, maximum, mean, median) of elemental concentrations ($ng.m^{-3}$) determined in PM_{10} by NAA

Element	Min	Max	Average	Median
Al	$1,15 \times 10^{-2}$	873,83	15,35	0,73
As	$5,84 \times 10^{-4}$	5,17	0,34	0,04
Ba	$4,63 \times 10^{-2}$	350,98	18,76	0,52
Br	$3,08 \times 10^{-4}$	1,72	0,18	0,12
Ca	$8,78 \times 10^{-1}$	87,38	13,47	7,33
Ce	$6,47 \times 10^{-3}$	1,01	0,12	0,07
Cl	$5,39 \times 10^{-2}$	150,66	15,73	2,12
Co	$1,71 \times 10^{-4}$	0,247	0,019	0,011
Cr	$4,30 \times 10^{-3}$	3,22	0,39	0,25
Cs	$9,64 \times 10^{-5}$	0,023	0,005	0,003
Eu	$3,39 \times 10^{-5}$	$1,90 \times 10^{-2}$	$3,26 \times 10^{-3}$	$1,60 \times 10^{-3}$
Fe	$2,15 \times 10^{-1}$	92,77	19,32	13,42
Hf	$5,49 \times 10^{-4}$	0,121	0,013	0,004
I	$7,19 \times 10^{-4}$	0,64	0,09	0,05
K	5,42	524,77	74,20	46,06
La	$4,37 \times 10^{-4}$	0,67	0,04	0,01
Mg	$3,65 \times 10^{-1}$	163,72	9,54	5,77
Mn	$1,18 \times 10^{-3}$	11,77	1,18	0,62
Na	$1,30 \times 10^{-1}$	1074,73	62,80	1,58
Rb	$3,02 \times 10^{-3}$	0,666	0,057	0,028
Sb	$4,73 \times 10^{-5}$	0,198	0,050	0,035
Sc	$3,18 \times 10^{-4}$	0,021	0,003	0,002
Se	$1,80 \times 10^{-4}$	0,176	0,022	0,012
Si	$1,69 \times 10^{1}$	6423,41	1529,79	1077,04
Sm	$2,51 \times 10^{-5}$	$6,35 \times 10^{-2}$	$2,65 \times 10^{-3}$	$7,44 \times 10^{-4}$
Sr	$6,01 \times 10^{-2}$	5,428	0,847	0,486
Ta	$1,55 \times 10^{-6}$	$1,94 \times 10^{-3}$	$2,36 \times 10^{-4}$	$1,23 \times 10^{-4}$
Tb	$3,06 \times 10^{-5}$	$6,54 \times 10^{-3}$	$8,90 \times 10^{-4}$	$5,75 \times 10^{-4}$
Th	$2,57 \times 10^{-4}$	$2,90 \times 10^{-2}$	$3,67 \times 10^{-3}$	$1,97 \times 10^{-3}$
U	$9,78 \times 10^{-5}$	$1,51 \times 10^{-1}$	$4,96 \times 10^{-3}$	$7,31 \times 10^{-4}$
V	$2,42 \times 10^{-4}$	0,191	0,027	0,018
W	$8,41 \times 10^{-4}$	0,202	0,012	0,007
Zn	$1,39 \times 10^{-2}$	729,39	40,84	0,16
Zr	$2,28 \times 10^{-2}$	7,14	1,04	0,80

Table 6: Elements with Pearson correlation coefficients > 0.7 for the respective seasons.

Warm season						**Cold season**						
As	Cl	Cr	I	Mg		**As**	La	Sm	Sr	U		
Ba	Zn					**Ba**	Ce	Rb	Sc	Sm	Ta	U
Br	Fe	La	Mn	Sm	Th	**Br**	I					
Ca	K					**Ce**	Rb	Sc	Ta	Th	U	Zr
Ce	K	Rb	Th			**Fe**	Sc					
Cl	Cr	I	Mg			**I**	Sb	Se				
Cr	I	Mg				**K**	Na					
Fe	Sm	Th				**La**	Sr					
Hf	Si					**Rb**	Sc	Ta	U			
I	Mg					**Sb**	Se					
La	Sm	Th				**Sc**	Ta					
Rb	Sm					**Sm**	U					
Sm	Th					**Ta**	U					
Ta	V											

Elemental contents and concentrations vary depending on the season. The data were therefore evaluated separately.

The correlation of the content of the determined elements depends on the season, which confirms the variability of the sources and the different origin of the pollution. A strong positive correlation ($R > 0.7$) was found between As and Cr, Mn, Br in the warm season and As correlated also with La, Sm, Sr and U in winter. This indicates - together with the directionality of the concentrations of these elements - that the occurrence of As in the warm season is related to metallurgical processes (Bureš and Velíšek 2005; Alleman et al. 2010; Sylvestre et al. 2017), whereas its source in winter samples is more likely to be coal combustion (Bures and Velíšek 2005; Hurst et al. 1991; Ritz et al. 2003; Horák et al. 2019; Ramme and Tharaniyil 2013; Robl et al. 2017).

In this study, the elemental content of coal combustion products, or more specifically, fly ash, plays an important role in determining the origin of pollution, especially in the cold season. The distribution of elements during this process has been well described in many papers (Ritz et al. 2003; Ramme and Tharaniyil 2013; Robl et al. 2017; Juda-Rezler and Kowalczyk 2013) and a number of factors needs to be taken into account. These include the contents of elements in the coal and their bonding, the boiling temperatures of the elements and their compounds (related to the combustion temperature). Other important factors influencing the resulting emissions are also the type of furnace, rated power, combustion temperature, type of separator and its operating temperature, physical-chemical reactions with other substances (additives, sulphur or halogens) and others. Depending on these conditions, different elemental compositions of fly ash emissions are described in the literature (Ritz et al. 2003; Wang et al. 2019; Bray et al. 2019; Pernigotti et al. 2016; Simon et al. 2010). The elements present in bituminous coal fly ash reported in most information sources are As, Cd, Se, Pb and Hg; other elements vary. Thus, the named elements can be considered as strong markers of the process. In view of the above limitations of NAA, other less common elements need to be investigated. Thus, the elemental composition of emissions from specific sources in the region was taken into account when determining the main sources of pollution based on other elements (Bureš and Velíšek 2005; Horák et al. 2019). Thus, the presence or absence of an element can indicate or exclude the origin of a particular source.

In the warm season, Fe was strongly correlated with Br, Sm and Th, while in winter only with Sc. Given the direction from which the highest concentrations of these elements (E, NE) originate, it can be assumed that their occurrence is related to primary metallurgy (Bureš and Velíšek 2005; Alleman et al. 2010). Cr correlated with As, I and Mg in the warm season too, while no significant correlation was found for winter samples. The highest concentrations of these elements in the warm season came from the west, suggesting a relation with steel and iron production (Sylvestre et al. 2017; Ghosh and Chatterjee 2010; Mohiuddin et al. 2014). For further correlations see Table 6 above. It should be noted that the REE values were well correlated, which is important both for assessing data quality and for understanding the process of pollution transfer (Beijer 1986; Avino et al. 2008)

A special attention was paid to the samples with the highest PM_{10} concentrations. The sample collected in August 2018 from the western sector was characterized by high concentrations of Cr, Mg and I (the highest of all the sets) and relatively high concentrations of Mn and Co. Cr and Co are important solutes for steel alloying; both Cr and Mg are important components of the refractory lining of metallurgical facilities (Ghosh and Chatterjee 2010; Bažan and Socha 2013). In addition, Mg (with Ca) is an essential additive used in almost every step of the steelmaking process from sintering and blast furnaces (dolomitic limestone, dolomite) to final steelmaking (magnesite). Mn is a common element in austenitic steels produced in local steelworks (Bureš and Velíšek 2005; Sylvestre et al. 2017; Ghosh and Chatterjee 2010; Bažan and Socha 2013). The presence of iodine may be related to coking (Bureš and Velíšek 2005). Given these facts, the steelworks west of the monitoring station is the most likely source of this peak PM_{10} concentration (see Figure 7 above).

The elemental composition of the sample from the south in February 2019 was characterized by high concentrations of Ca, Se and V (the highest of all the sets) and relatively high concentrations of I and Sb. The high Ca concentration is probably related to the cement plant (Bureš and Velíšek 2005; Larsen et al. 2012; Samara et al. 2003; Yatkin and Bayram 2008), and given the meteorological conditions mentioned above, this high peak concentration likely came from the cement plant relatively far from the sampling tower (about 50 km to the southwest). This hypothesis can be supported by the fact that alternative fuels based on waste or tar, in addition to coal, are used in the clinker firing at this plant, which may explain the high concentrations of the other determined elements.

Samples collected during smog events varied significantly in their elemental composition. The PM_{10} samples collected in November 2018 were characterized by high concentrations of Ba, Ce, Fe, Hf, Rb, Sc, Ta, Th, U and Zr (the highest of all samples), while the sample in March 2019 was characterized by high concentrations of Si, Sr, Zn and Eu. The elemental composition of the first sample suggests two sources of pollution: coal combustion and metallurgy (Seibert et al. 2020; Bures and Velíšek 2005; Sylvestre et al. 2017; Horák et al. 2019). These high concentrations were collected during steady airflow from NE, E and SE directions, suggesting the origin of pollution in the steelworks to the southeast to the sampling location (see Figure 7), along with coal combustion in local furnaces. The origin of pollution in the second inversion is not as clear; however, the modelled airflow directs towards the Polish border region (see Figure 61) (Bures and Velíšek 2005; Ritz et al. 2003; Mohiuddin et al. 2014; Larsen et al. 2012).

7.3 Summary of PM measurements

In this activity, the elemental composition of the collected PM_{10} was determined using NAA and the origin of the pollution was explained on the basis of the determined elemental composition as an indicator of pollution sources, statistical analyses and meteorological models. More often, the origin of pollution is investigated using receptor modelling (Pokorná et al. 2015; Seibert et al. 2020; Norris et al. 2014; European Commission. Joint Research Centre. 2019; Samara et al. 2003). Considering the specifics of the obtained dataset (long sampling period, small number of samples in each sector), irregular temporal resolution of the samples and questionable construction of the uncertainty matrix (different weights of the respective samples), the use of this method is not adequate.

Despite the described limitations of the applied methods, this work confirmed that pollution in the region is influenced by specific types of pollution sources, including two metallurgical plants (west and southeast of the sampling site), which under certain meteorological conditions increase the pollution load in the region and contribute to the transfer of pollution in the upper atmosphere. In certain situations, however, this transfer is not detected by ground monitoring stations (compared to (Czech Hydrometeorological Institute 2018)). This confirms the justification for locating the sampling device at 90 m above the ground surface. By sampling at such a height, the contribution of local sources (household emissions, traffic, construction activities, autumn biomass burning, etc.) is excluded (Seibert et al. 2020; Bernardoni et al. 2011; Cristina Colombi et al. 2010) and pollution transfer in the region can be defined more accurately.

The second specific type of pollution in the region is pollution related to transboundary transfer from Poland originating from the coal burning in domestic boilers during the winter season. During the cold part of the year, PM_{10} concentrations originating from the Polish border region (from the north, north-east and east directions) increased by almost 50%, despite the fact that the prevailing wind direction was, according to the ground observations, exactly the opposite. This fact has already been reported in many previous studies (Blažek 2013; Jančík et al. 2013; Czech Hydrometeorological Institute 2019; Seibert et al. 2020; Černikovský et al. 2016). However, measurements at the towertop showed that the prevailing flow direction during the cold part of the year was northeast and north, i.e. just from the Polish side. Thus, this finding may change the perspective on the interpretation of pollution transfer within the region. These results again confirm the importance of the transboundary influence on PM concentrations in the region and point out at the fact that this is not only a problem of the nearby border area, but of the region as a whole.

Neutron activation analysis was used to determine the elemental composition of the samples and a wide range of elements was determined. Although this method presented some limitations, it definitely helped to identify the origin of the elemental concentrations in the samples by determining the concentrations of less common elements. Although it should be noted that NAA does not provide data on some important elements such as Cd, Cu, Hg or Pb, the information obtained was in most cases sufficient to identify the source of the pollution.

In order to collect more data on the transfer of pollution in the area during different meteorological years and to refine the assessment, monitoring at the measuring devices goes on.

8 CONCLUSION

The joint Czech-Polish measurements of transboundary transfer of air pollutants presented in this monograph were carried out as part of the project of the same name with the acronym "AIR BORDER". The aim of the measurements was to better understand the pollution originating from cross-border transmission and to describe in more detail the process of PM_{10} transfer within the area of interest. Therefore, the air pollution by suspended particles and meteorological data were measured at stations on both sides of the border. On the Czech side, measurements were performed at the newly established station in Horní Suchá in the František industrial zone, and on the Polish side at the existing IMWM-SRI station in Racibórz.

Concentrations of suspended particles of PM_1, $PM_{2.5}$, PM_{10} fractions and total suspended particles (TSP) and basic meteorological characteristics – temperature, pressure, humidity, wind speed and direction – were continuously measured at both localities. The station in Racibórz was further equipped with a device for continuous measurement of the vertical temperature profile in the atmospheric boundary layer with the aim to identify the inversion layer of air pollution dispersion, as a key factor in the transmission of pollution in the open atmosphere (Blažek 2013; Volná and Hladký 2020). Its primary purpose was therefore to monitor the transmission of pollution in terms of meteorological parameters. The station in Horní Suchá was more focused on the identification of the particles themselves.

Monitoring in Horní Suchá observed the transmission of suspended particle pollution in an effort to exclude the influence of local sources (Volná and Hladký 2020). To this aim, a specially designed high-volume sampler (SAM Hi 30 AUTO WIND) was used for sampling. The sampler was placed on the top of a former mining tower at a height of approximately 90 m above the ground level. This made it possible to study the regional transmission of pollution and at the same time to meet the assumption of excluding the influence of local sources. The elemental composition of the collected particles was determined by neutron activation analysis and the results were used together with the determined PM_{10} concentrations and meteorological data (measured and modeled) to identify the origin of pollution in the area. A significant difference in the composition of the elements was observed: the concentrations of the elements depended on both the season and the sampling direction. Situations were identified where the pollution came from specific sources of pollution in the area.

The project's monitoring of meteorological parameters against the background of long-term measurements showed that in the evaluated years 2018 and 2019, dispersion conditions were extremely favorable and the winters were relatively mild in the area. From this, it follows that the area saw a lower burden of emissions from local furnaces during the heating season. This was also reflected in the concentrations of measured suspended PM particles in the given period. In terms of meteorological conditions in the area, it can be stated that the observed period was abnormal and that it is desirable to continue the joint research to gain a deeper understanding of pollution transfer processes. Observations made using specialized meteorological equipment acquired in the scope of the project at the station in Racibórz, in combination with measurements at the station on the tower in Horní Suchá at an altitude of approx. 90 m AGL, revealed situations where the prevailing wind direction (and thus pollution transfer) at the ground layer was different, or completely opposite to that above the inversion layer. This finding shows that there are situations, especially at high concentrations of pollution, where standardly operated air quality monitoring stations are not able to capture the complexity of cross-border transmission of pollution and thus correctly interpret its origin. This proves the necessity and justification of the use of the acquired equipment, together with the need for its subsequent operation and the evaluation of measured data.

Based on the results of the AIR BORDER project, the design of which is summarized in this monograph, it is possible to better understand the process of cross-border transfer of pollutants, including the factors that affect it. This information can then serve as a basis in the creation of tools leading to the solution of unfavorable air quality in the region and the implementation of specific measures. Given the location of the area of interest, cooperation between the professional and lay public, including political representation, will be necessary to address the problem of air pollution.

9 REFERENCES

ALLEMAN, Laurent Y., Laure LAMAISON, Esperanza PERDRIX, Antoine ROBACHE a Jean-Claude GALLOO, 2010. PM_{10} metal concentrations and source identification using positive matrix factorization and wind sectoring in a French industrial zone. Atmospheric Research [online]. 96(4), 612–625. ISSN 01698095. Available online: doi:10.1016/j.atmosres.2010.02.008

AVINO, P., G. CAPANNESI a A. ROSADA, 2008. Heavy metal determination in atmospheric particulate matter by Instrumental Neutron Activation Analysis. Microchemical Journal [online]. 88(2), SELECTED PAPERS FROM THE 1st INTERNATIONAL SYMPOSIUM ON MULTIVARIATE ANALYSIS AND CHEMOMETRICS FOR CULTURAL HERITAGE AND ENVIRONMENT Nemi, Italy 2 - 4 October 2006, 97–106. ISSN 0026-265X. Available online: doi:10.1016/j.microc.2007.11.005

BAŽAN, Jiří a Ladislav SOCHA, 2013. ZÁKLADY TEORIE A TECHNOLOGIE VÝROBY ŽELEZA A OCELI: Část II - Základy teorie a technologie výroby oceli. 1. Ostrava, Czech Republic: VŠB – Technická univerzita Ostrava. ISBN 978-80-248-3353-8. (in Czech)

BEIJER, K, 1986. Sources, transport and transformation of metals in the environment. Handbook of the Toxicology of Metals. 1, 68.

BERNARDONI, Vera, Roberta VECCHI, Gianluigi VALLI, Andrea PIAZZALUNGA a Paola FERMO, 2011. PM_{10} source apportionment in Milan (Italy) using time-resolved data. Science of The Total Environment [online]. 409(22), 4788–4795. ISSN 00489697. Available online: doi:10.1016/j.scitotenv.2011.07.048

BLAŽEK, Zdeněk, ed., 2013. Vliv meteorologických podmínek na kvalitu ovzduší v přeshraniční oblasti Slezska a Moravy =: Wpływ warunków meteorologicznych na jakość powietrza w obszarze przygranicznym Śląska i Moraw = The influence of meteorological conditions on air quality in the border region of Silesia and Moravia [online]. Vydání první. Praha : Warszawa: Český hydrometeorologický ústav ; Instytut Meteorologii i Gospodarki Wodnej, Państwowy Instytut Badawczy. ISBN 978-80-87577-15-8. Available online: http://portal.chmi.cz/files/portal/docs/poboc/OS/OCO/pdf_ooco/publikace.pdf (in Czech / in Polish)

BRAY, Casey D., Madeleine STRUM, Heather SIMON, Lee RIDDICK, Mike KOSUSKO, Marc MENETREZ, Michael D. HAYS a Venkatesh RAO, 2019. An assessment of important SPECIATE profiles in the EPA emissions modeling platform and current data gaps. Atmospheric Environment [online]. 207, 93–104. ISSN 13522310. Available online: doi:10.1016/j.atmosenv.2019.03.013

BUREŠ, Vladimír a Jan VELÍŠEK, 2005. Reduction of emissions of pollutants into the air: 2nd stage, year 2005 (Omezování emisí znečišťujících látek do ovzduší: II. etapa, rok 2005) [online]. listopad 2005. B.m.: TECHNICKÉ SLUŽBY OCHRANY OVZDUŠÍ PRAHA, a.s. Available online: http://www.teso.cz/adm/data/files/others/zprava-vav-sm-9_14_04-2005.pdf (in Czech)

CARSLAW, David a Karl ROPKINS, 2020. Package ‘openair’ [online]. 06 2020. Available online: https://cran.r-project.org/web/packages/openair/openair.pdf

CRISTINA COLOMBI, VORNE GIANELLE, CLAUDIO BELIS, a BO LARSEN, 2010. Determination of local source profile for soil dust, brake dust and biomass burning sources. Chemical Engineering Transactions [online]. 22, 233–238. Available online: doi:10.3303/CET1022038

CZECH HYDROMETEOROLOGICAL INSTITUTE, 2018. CHMI - Tabular survey, air pollution and atmospheric deposition in data, the Czech republic - 2017. Czech Hydrometeorological Institute [online] [vid. 2020-04-14]. Available online: https://www.chmi.cz/files/portal/docs/uoco/isko/tab_roc/2017_enh/index_GB.html

CZECH HYDROMETEOROLOGICAL INSTITUTE, 2019. CHMI - Tabular survey, air pollution and atmospheric deposition in data, the Czech republic - 2018. Czech Hydrometeorological Institute [online] [vid. 2020-04-14]. Available online: http://portal.chmi.cz/files/portal/docs/uoco/isko/tab_roc/2018_enh/index_GB.html

CZECH HYDROMETEOROLOGICAL INSTITUTE, 2020. CHMI - Tabular survey, air pollution and atmospheric deposition in data, the Czech republic - 2019. Czech Hydrometeorological Institute [online] [vid. 2020-04-14]. Available online: https://www.chmi.cz/files/portal/docs/uoco/isko/tab_roc/2019_enh/index_GB.html

ČESKÝ HYDROMETEOROLOGICKÝ ÚSTAV a UNIVERZITA PALACKÉHO V OLOMOUCI, 2007. Atlas podnebí Česka (Climate atlas of Czechia). Vydání 1. Praha : Olomouc: Český hydrometeorologický ústav ; Univerzita Palackého v Olomouci. ISBN 978-80-86690-26-1. (in Czech)

DEGÓRSKA, Anna, Katarzyna JUDA-REZLER a Barbara TOCZKO, ed., 2016. Pyły drobne w atmosferze: kompendium wiedzy o zanieczyszczeniu powietrza pyłem zawieszonym w Polsce: praca zespołowa [online]. 1. Warszawa: Główny Inspektorat Ochrony Środowiska. ISBN 978-83-61227-73-1. Available online: https://www.gios.gov.pl/images/aktualnosci/Pyly_drobne_w_atmosferze.Kompendium_wiedzy.pdf (in Polish)

EUROPEAN COMMISSION. JOINT RESEARCH CENTRE., 2019. European guide on air pollution source apportionment with receptor models: revised version 2019. [online]. LU: Publications Office [vid. 2020-12-02]. Available online: https://data.europa.eu/doi/10.2760/439106

EUROPEAN COMMITTEE FOR STANDARDIZATION, 2014. EN 12341:2014 - Ambient air - Standard gravimetric measurement method for the determination of the PM_{10} or $PM_{2.5}$ mass concentration of suspended particulate matter. 2014. B.m.: European Committee for Standardization.

EUROPEAN COUNCIL, 2008. Directive 2008/50/EC of the European Parliament and of the Council of 21 May 2008 on ambient air quality and cleaner air for Europe [online]. 11. červen 2008. [vid. 2020-04-14]. Available online: https://eur-lex.europa.eu/legal-content/EN/TXT/?uri=OJ:L:2008:152:TOC

FRONTASYEVA, M. V., S. S. PAVLOV a V. N. SHVETSOV, 2010. NAA for applied investigations at FLNP JINR: present and future. Journal of Radioanalytical & Nuclear Chemistry [online]. 286(2), 519–524. ISSN 02365731. Available online: doi:10.1007/s10967-010-0814-z

GHOSH, Ahindra a Amit CHATTERJEE, 2010. Ironmaking and steelmaking: theory and practice. 3. print. New Delhi: PHI Learning. Eastern economy edition. ISBN 978-81-203-3289-8.

HORÁK, Jiří, Lenka KUBOŇOVÁ, Stanislav BAJER, Milan DEJ, František HOPAN, Kamil KRPEC a Tadeáš OCHODEK, 2019. Composition of ashes from the combustion of solid fuels and municipal waste in households. Journal of Environmental Management [online]. 248, 109269. ISSN 03014797. Available online: doi:10.1016/j.jenvman.2019.109269

HURST, Richard W., Terry E. DAVIS a Ahmed A. ELSEEWI, 1991. Strontium isotopes as tracers of coal combustion residue in the environment. Engineering Geology [online]. 30(1), Applied Geosciences for Low-Level Radioactive and Chemical Wastes, 59–77. ISSN 0013-7952. Available online: doi:10.1016/0013-7952(91)90035-J

INMETEO, 2020. VENTUSKY. VENTUSKY [online]. Available online: https://www.ventusky.com/?p=49.8;18.5;5&l=wind-10m

JIŘÍK, Vítězslav, Barbara HERMANOVÁ, Andrea DALECKÁ, Irena PAVLÍKOVÁ, Jan BITTA, Petr JANČÍK, Leszek OŚRÓDKA, Ewa KRAJNY, Franciszek SŁADECZEK, Grzegorz SIEMIĄTKOWSKI, Katarzyna KIPRIAN a Ewa GŁODEK BUCYK, 2020. Wpływ zanieczyszczenia powietrza na zdrowie ludności w obszarze polsko-czeskiego pogranicza / Dopad znečištění ovzduší na zdravotní stav obyvatelstva v česko-polském příhraničí [online]. 1. B.m.: Sieć Badawcza Łukasiewicz – Instytut Ceramiki i Materiałów Budowlanych Instytut Meteorologii i Gospodarki Wodnej – Państwowy Instytut Badawczy Ostravská univerzita Vysoká škola báňská – Technická univerzita Ostrava. ISBN ISBN 978-80-248-4406-0. Available online: https://healthair.eu/images/PDF/Publikacja_podsumowująca/Publikacja%20Healthair.pdf ((in Czech / in Polish)

JUDA-REZLER, Katarzyna a Dominik KOWALCZYK, 2013. Size Distribution and Trace Elements Contents of Coal Fly Ash from Pulverized Boilers. Polish Journal of Environmental Studies. 22(1), 25–40. ISSN 1230-1485.

KOTTEK, Markus, Jürgen GRIESER, Christoph BECK, Bruno RUDOLF a Franz RUBEL, 2006. World Map of the Köppen-Geiger climate classification updated. Meteorologische Zeitschrift [online]. 15(3), 259–263. ISSN 0941-2948. Available online: doi:10.1127/0941-2948/2006/0130

KRAJNY, Ewa a Leszek OŚRÓDKA, 2020. Sprawozdanie z realizacji zadań statutowych DS.-M3/2019 Opracowanie modułu imisji stężeń zanieczyszczeń powietrza Wykorzystanie wybranych metod teledetekcji naziemnej doskonalenia diagnozy i prognozy jakości powietrza. 2020. B.m.: Instytut Meteorologii i Gospodarki Wodnej – Państwowy Instytut Badawczy. (in Polish)

KRUG, Jonathan D., Andrew DART, Carlton L. WITHERSPOON, Jerome GILBERRY, Quentin MALLOY, Surender KAUSHIK a Robert W. VANDERPOOL, 2017. Revisiting the size selective performance of EPA's high-volume total suspended particulate matter (Hi-Vol TSP) sampler. Aerosol Science and Technology [online]. 51(7), 868–878. ISSN 0278-6826, 1521-7388. Available online: doi:10.1080/02786826.2017.1316358

KURFÜRST, Jiří, 2008. Kompendium ochrany kvality ovzduší. Chrudim: Vodní zdroje Ekomonitor. ISBN 978-80-86832-38-8.

LARSEN, B.R., S. GILARDONI, K. STENSTRÖM, J. NIEDZIALEK, J. JIMENEZ a C.A. BELIS, 2012. Sources for PM air pollution in the Po Plain, Italy: II. Probabilistic uncertainty characterization and sensitivity analysis of secondary and primary sources. Atmospheric Environment [online]. 50, 203–213. ISSN 13522310. Available online: doi:10.1016/j.atmosenv.2011.12.038

MOHIUDDIN, K., V. STREZOV, P. F. NELSON a E. STELCER, 2014. Characterisation of trace metals in atmospheric particles in the vicinity of iron and steelmaking industries in Australia. Atmospheric Environment [online]. 83, 72–79. ISSN 1352-2310. Available online: doi:10.1016/j.atmosenv.2013.11.011

NORRIS, Gary, Rachelle DUVALL, Steve BROWN a Song BAI, 2014. Positive Matrix Factorization (PMF) 5.0 Fundamentals and User Guide [online]. duben 2014. B.m.: United States Environmental Protection Agency. Available online: https://www.epa.gov/sites/production/files/2015-02/documents/pmf_5.0_user_guide.pdf

OŚRÓDKA, Leszek, Ewa KRAJNY a Marek WOJTYLAK, 2018. Application of the Data Mining Methods to Assess the Impact of Meteorological Conditions on the Episodes of High Concentrations of PM_{10} along the Polish – Czech Border. E3S Web of Conferences [online]. 28, 01027. ISSN 2267-1242. Available online: doi:10.1051/e3sconf/20182801027

PAVLÍKOVÁ, Irena, Daniel HLADKÝ, Oldřich MOTYKA, Konstantin N. VERGEL, Ludmila P. STRELKOVA a Margarita S. SHVETSOVA, 2020. Characterization of PM_{10} Sampled on the Top of a Former Mining Tower by the High-Volume Wind Direction-Dependent Sampler Using INNA. Atmosphere [online]. 12(1), 29. ISSN 2073-4433. Available online: doi:10.3390/atmos12010029

PAVLOV, Sergey, Andrey DMITRIEV a Marina FRONTASYEVA, 2016. Automation system for neutron activation analysis at the reactor IBR-2, Frank Laboratory of Neutron Physics, Joint Institute for Nuclear Research, Dubna, Russia. Journal of Radioanalytical & Nuclear Chemistry [online]. 309(1), 27–38. ISSN 02365731. Available online: doi:10.1007/s10967-016-4864-8

PERNIGOTTI, Denise, Claudio A. BELIS a Luca SPANÒ, 2016. SPECIEUROPE: The European data base for PM source profiles. Atmospheric Pollution Research [online]. 7(2), 307–314. ISSN 13091042. Available online: doi:10.1016/j.apr.2015.10.007

POKORNÁ, P., J. HOVORKA, M. KLÁN a P. K. HOPKE, 2015. Source apportionment of size resolved particulate matter at a European air pollution hot spot. The Science of the Total Environment [online]. 502, 172–183. ISSN 1879-1026. Available online: doi:10.1016/j.scitotenv.2014.09.021

R STUDIO, 2020. Package 'ggplot2' [online]. 06 2020. Available online: https://cran.r-project.org/web/packages/ggplot2/ggplot2.pdf

RAMME, Bruce W. a Mathew P. THARANIYIL, 2013. Coal Combustion Products Utilization Handbook [online]. 3rd Edition. Milwaukee, United States of America: We Energies. Available online: https://www.we-energies.com/environmental/ccp_handbook.pdf

RITZ, Michal, Lucie BARTOŇOVÁ a Zdeněk KLIKA, 2003. EMISSIONS OF HEAVY METALS AND POLYAROMATIC HYDROCARBONS DURING COAL COMBUSTION IN INDUSTRIAL AND SMALL SCALE FURNACES (EMISE TĚŽKÝCH KOVŮ A POLYAROMATICKÝCH UHLOVODÍKŮ PŘI SPALOVÁNÍ UHLÍ V PRŮMYSLOVÝCH A MALÝCH TOPENIŠTÍCH). Sborník vědeckých prací Vysoké školy báňské – Technické univerzity Ostrava. 2003(1), Řada hornicko-geologická, 69–82. ISSN ISSN 0474-8476. (in Czech)

ROBL, Thomas L., Anne OBERLINK a Rod JONES, ed., 2017. Coal combustion products (CCPs): characteristics, utilization and beneficiation. Duxford, United Kingdom ; Cambridge, Massachusetts: Woodhead Publishing, an imprint of Elsevier. Woodhead series in energy. ISBN 978-0-08-100945-1.

ROLPH, Glenn, Ariel STEIN a Barbara STUNDER, 2017. Real-time Environmental Applications and Display sYstem: READY. Environmental Modelling & Software [online]. 95, 210–228. ISSN 13648152. Available online: doi:10.1016/j.envsoft.2017.06.025

SAMARA, C, Th KOUIMTZIS, R TSITOURIDOU, G KANIAS a V SIMEONOV, 2003. Chemical mass balance source apportionment of PM_{10} in an industrialized urban area of Northern Greece. Atmospheric Environment [online]. 37(1), 41–54. ISSN 13522310. Available online: doi:10.1016/S1352-2310(02)00772-0

SEIBERT, Radim, Irina NIKOLOVA, Vladimíra VOLNÁ, Blanka KREJČÍ a Daniel HLADKÝ, 2020. Air Pollution Sources' Contribution to $PM_{2.5}$ Concentration in the Northeastern Part of the Czech Republic. Atmosphere [online]. 11(5), 522. Available online: doi:10.3390/atmos11050522

SIMON, Heather, Lee BECK, Prakash V. BHAVE, Frank DIVITA, Ying HSU, Deborah LUECKEN, J. David MOBLEY, George A. POULIOT, Adam REFF, Golam SARWAR a Madeleine STRUM, 2010. The development and uses of EPA's SPECIATE database. Atmospheric Pollution Research [online]. 1(4), 196–206. ISSN 1309-1042. Available online: doi:10.5094/APR.2010.026

STEIN, A. F., R. R. DRAXLER, G. D. ROLPH, B. J. B. STUNDER, M. D. COHEN a F. NGAN, 2015. NOAA's HYSPLIT Atmospheric Transport and Dispersion Modeling System. Bulletin of the American Meteorological Society [online]. 96(12), 2059–2077. ISSN 0003-0007, 1520-0477. Available online: doi:10.1175/BAMS-D-14-00110.1

SYLVESTRE, Alexandre, Aurélie MIZZI, Sébastien MATHIOT, Fanny MASSON, Jean L. JAFFREZO, Julien DRON, Boualem MESBAH, Henri WORTHAM a Nicolas MARCHAND, 2017. Comprehensive chemical characterization of industrial $PM_{2.5}$ from steel industry activities. Atmospheric Environment [online]. 152, 180–190. ISSN 13522310. Available online: doi:10.1016/j.atmosenv.2016.12.032

UNITED STATES ENVIRONMENTAL PROTECTION AGENCY, 1999. Compendium of Methods for the Determination of Inorganic Compounds in Ambient Air: SAMPLING OF AMBIENT AIR FOR TOTAL SUSPENDED PARTICULATE MATTER (SPM) AND PM_{10} USING HIGH VOLUME (HV) SAMPLER [online]. červen 1999. B.m.: United States Environmental Protection Agency. Available online: https://www.epa.gov/sites/production/files/2015-07/documents/epa-io-2.1.pdf

UNITED STATES ENVIRONMENTAL PROTECTION AGENCY, OFFICE OF AIR AND RADIATION, a OFFICE OF AIR QUALITY PLANNING AND STANDARDS, 2000. Meteorological Monitoring Guidance for Regulatory Modeling Applications [online]. únor 2000. B.m.: UNITED STATES ENVIRONMENTAL PROTECTION AGENCY. Available online: https://www3.epa.gov/scram001/guidance/met/mmgrma.pdf

VOLNÁ, Vladimíra a Daniel HLADKÝ, 2020. Detailed Assessment of the Effects of Meteorological Conditions on PM_{10} Concentrations in the Northeastern Part of the Czech Republic. Atmosphere [online]. 11(5), 497. ISSN 2073-4433. Available online: doi:10.3390/atmos11050497

WANG, Jinxi, Zhen YANG, Shenjun QIN, Balaji PANCHAL, Yuzhuang SUN a Hongya NIU, 2019. Distribution characteristics and migration patterns of hazardous trace elements in coal combustion products of power plants. Fuel [online]. 258, 116062. ISSN 00162361. Available online: doi:10.1016/j.fuel.2019.116062

YATKIN, Sinan a Abdurrahman BAYRAM, 2008. Determination of major natural and anthropogenic source profiles for particulate matter and trace elements in Izmir, Turkey. Chemosphere [online]. 71(4), 685–696. ISSN 00456535. Available online: doi:10.1016/j.chemosphere.2007.10.070

ZDARBUH.CZ, 2020. Kouře ve výdušné jámě na Dole Prezident Gottwald v Horní Suché 21. února 1983 | Zdař Bůh.cz. Zdař Bůh.cz [online]. [vid. 2021-09-08]. Available online: https://www.zdarbuh.cz/reviry/okd/koure-ve-vydusne-jame-na-dole-prezident-gottwald-v-horni-suche-21-unora-1983/ (in Czech)

ZIEMIAŃSKI, Michał a Leszek OŚRÓDKA, ed., 2012. Zmiany klimatu a monitoring i prognozowanie stanu środowiska atmosferycznego [online]. Warszawa: Instytut Meteorologii i Gospodarki Wodnej, Państwowy Instytut Badawczy. Wpływ zmian klimatu na środowisko, gospodarkę i społeczeństwo : zmiany, skutki i sposoby ich ograniczenia, wnioski dla nauki, praktyki inżynierskiej i planowania gospodarczego, tom 2. ISBN 978-83-61102-66-3. Available online: https://www.imgw.pl/sites/default/files/2020-08/klimat-tom-ii-zmiany-klimatu-a-monitoring-i-prognozowanie-stanu-srodowiska-atmosferycznego-min.pdf (in Polish)

PROJECT PARTNERS

VŠB TECHNICKÁ UNIVERZITA OSTRAVA

IMGW

BEZPEČNOSTNĚ TECHNOLOGICKÝ KLASTR

PUBLISHES

VSB - Technical University of Ostrava
17. listopadu 2172/15 Ostrava - Poruba 708 00
ISBN 978-80-248-4550-0